Glass Beads, Markers of Ancient Trade in Sub-Saharan Africa: Methodology, State of the Art and Perspectives

Farahnaz Koleini, Philippe Colomban, Innocent Pikirayi, Linda Prinsloo

Glass beads, markers of ancient trade in Africa: methodology, state of the art and perspectives

Farahnaz Koleini[1], Philippe Colomban[2], Innocent Pikirayi[1], Linda C. Prinsloo[3]

[1]*Department of Anthropology and Archaeology, Faculty of Humanities, University of Pretoria, Pretoria, Gauteng, South Africa.*

[2] *Sorbonne Université, CNRS, MONARIS UMR8233, 4 Place Jussieu, 75005 Paris, France, ORCID:0000-0001-6099-5423*

[3] *School of Earth and Environmental Sciences, University of Wollongong, Wollongong, NSW 2522, Australia; Email: lprinslo@uow.edu.au*

**corresponding author:*

Abstract

Glass beads have been produced and traded for millennia all over the world, and used as everyday items of adornment, ceremonial costumes or objects of barter. The preservation of glass beads is good and large hoards have been found across the world. The variety of shape, size and colour as well as the composition and production technologies of glass beads motivated efforts to use them as markers of exchange pathways, from/around/through/to Indian Ocean, Africa, Asia, Middle East, Europe and America and as chronological milestones. This review addresses the methodology of identification (morphology, elemental composition, glass nanostructure, colouring and opacifying agents, and secondary phases) by means of laboratory and mobile instruments used on glass beads excavated from Southern Africa sites. The review concludes by discussing the potential information that could be extracted using advanced portable methods of analysis.

Keywords Trade. Beads. Glass. Pigments. Provenance. Africa. Asia. Mediterranean World

Introduction: overview of glass production history

The first long distance trade in obsidian, a natural hard and brittle volcanic glass that fractures with very sharp edges and used to make cutting and piercing tools, was established during Neolithic times [1,2]. The trade in synthetic glass objects and especially glass beads is not so old but covered really long distances, especially around and through the Indian Ocean. Since the beginning of the first millennium AD, mostly with the assistance of monsoon winds, the Indian Ocean was organized into a space around which the first World Trade system was built [3,4]; connecting the Near/Middle East, India, South Asia, China and Africa [5]. Europe started trading beads to Africa from the 15th century AD. European glass beads were also exported to America as early as the16th century [6-8].

The production of glazed artefacts is old, going back to 4000/5000 BC [9] and the first synthetic glass, or more precisely coloured glass paste (glassy faience) was made in Egypt, Mesopotamia and the Indus Valley circa 2000 BC to replace semiprecious stones and gems [10-12]. From about 1500 BC transparent glass artefacts were produced in the Levant, Crete and Egypt with a colour palette that broadened gradually until 1200 BC when a political unrest led to a dramatic break in glass production [13]. New achievements in glass making and production had to wait until the 9th century BC, when the production of an almost colourless glass commenced in Syria and Cyprus [14,15] and an up-graded moulding technique ("lost wax") made it possible to achieve new complex shapes and designs [16]. Around 200 BC, Roman glassmakers developed the blowing technique and the production of glass artefacts became a heavy industry around 50 BC.

Alexandria (Egypt), Sidon (Lebanon), Belus River (Levant), Campania, Rome (Italy) and Gaul (France) are mentioned as the most important industrial centres in Pliny the Elder's texts [17]. The most famous artefacts are enamelled glasses as those from the Begram Ptolemaic Treasure [18] dated from the late Roman Empire to the early Byzantine times [19]. Then, the Normand Court continued the production of complex enamelled objects [20] that developed during the Fatimid and Mamluk dynasties [21]. Enamelling and gilding declined in Near-East countries at the end of the Middle-Ages as a direct consequence of the decline of Islamic influence following the sack of Damascus by the Mongols [22] and of Byzantium by the Crusaders. The golden age of Venetian glass thus started [23,24]. Byzantine craftsmen

had already developed Venetian glass production by the 13th century after arriving in Venice following the sack of Byzantium. The highly skilled expertise of Venetian glassmakers reached its height by the 16th century when Murano workshops produced first *cristallo* (rock crystal-like) glass, *lattimo* (milky glass), aventurine glass and *millefiori.*

A decentralisation of glass production centres occurred during the Middle-Ages in western and northern European countries (for forest glass, see below); Cologne, Leuven, Namur, Amiens, and Beauvais became important sites [25]. By the 16th century *Façon de Venise* glass objects with the same transparency as original Venetian *cristallo* were produced in Holland [21]. During the 17th century, new kinds of clear, lead-based glasses were introduced. In England, G. Ravenscroft discovered the advantages of lead-based glass (*crystal* and *flint*-glass) with high optical index and easiness to form or mould. The so called *crystal* and of *flint*-glass were made of high purity raw materials [26,27]. At the same time Bohemian glassmakers prepared a lead-based glass, richer in potassium and calcium that made enamelling easier [28]. Lead glass became popular with Dutch glass engravers. The implementation of press-moulding in the USA (ca. 1825), the transfer painting and acid-etching, as well as new colouring agents enlarged the variety of glass [26,29].

Glass production in southern India, Thailand, Vietnam, Philippines and China seems to be started in 3000 ago [30-33]. Arikamedu is considered as the main and oldest Indian bead making site (a few centuries BC) [34] (Dussubieux et al. 2008). Its old name Virampatnam has been identified with Pôdouké Emporion mentioned in the ancient texts of Ptolemy and *Periplus Maris Erythraei* [5]. Other ancient sites of production are Mantai (old name *Modutti*), in Sri Lanka, Oc éo (*Kattigara*, Funan Kingdom) that is mentioned in Ptolemy Geography, in south of Vietnam, Khlong Thom, in Thailand and Kuala Selinsing, in Malaysia. In China the glass paste/glassy faience production dates from the Western Zhou Dynasty (~1000 BC), but glass production was mainly developed during the Warring States Period and then the Eastern Han Dynasty (~4th BC) in the provinces of Xingjian, Shandong, Henan, Guangdong and along the Yangtze River [33]. Two types of lead-based glass were produced, with barium or sodium as the other fluxing agent. Glass production in central Vietnam is documented for the Sa Huynh Culture (1000 to ~0 BC) [5] because of the development of firing techniques [35]. Although ancient glass production in Europe and Mediterranean world is archeologically well documented [9], that in Asian countries is still work in progress [36,37].

Glass objects differ in their shape because of aesthetic and cultural/commercial constraints and the morphology of an object are used by scholars as a criterion of dating and sourcing. Beads are among the first examples of humankind's creativity, together with stone tools and rock art. The first beads, dating more than 100,000-year-old, were made by piercing shells [38,39], and after that holes were drilled into polished or natural stones (e.g. steatite) and gems (e.g. carnelian). Glazed stone and synthetic faience were used in early kingdoms of Mesopotamia and Egypt. The preservation of glass beads is rather good and for instance Francis [5] tried to trace Asia's Indian Ocean trade by identifying beads and their production centres and his work was recently revisited [40-44].

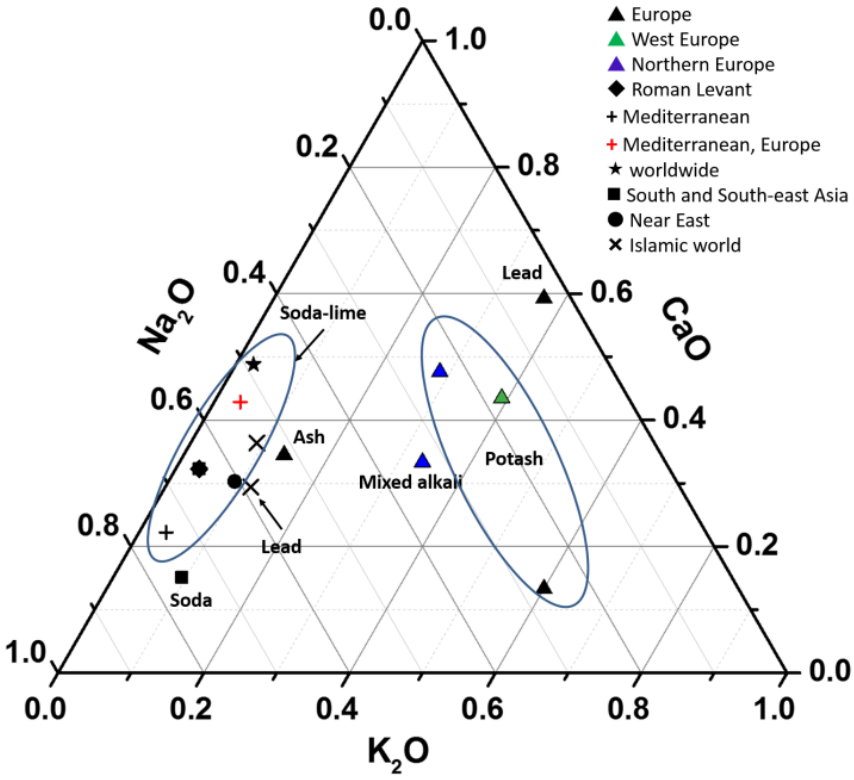

Fig. 1 Variety of the glass flux compositions expressed in the Na_2O-K_2O-CaO relative ratio.

The first glass beads were made by winding glass paste around a metal rod [45]. A better mastering of the glass melting and viscosity led to the manufacture of tubes, which are cut in beads, resulting in a variety of size and shapes. The moulding technique is ancient but developed further together with the spinneret technique during the industrial revolution [9].

Even though many protocols (see below in this section) to investigate the provenance of glass artefacts has been carried out [9,17,46] the multifaceted composition of a glass batch

(summarized in Figure 1 and Table 1) and the complex reactions that occur during melting, together with all aspects introduced through recycling, especially of coloured glasses, make the identification of historical sources difficult. In some cases, elements characteristics of a given type of raw material of a technology level can be searched. The alternative method is the use of algorithmic calculation such as Principal Component Analysis and Cluster Variation methods to identify correlations/relationships between different artefacts [44,47].

Table 1 Glass types, main characteristics and origin/period

Flux	Glass type	Sub-groups	Average oxide content wt%					Expected Alkali source	Period	Expected Origin
			Na_2O	K_2O	CaO	MgO	PbO			
Na	Soda	low Al							>2AD	South Asia, South-East Asia
		high Al (Al_2O_3:4-10)	15-20	1.5-2.5	2-4	0.2-1		?	> 1BC~-6AD	
									9-19AD	South Asia
		Venetian cristallo Façon de Venise	12-15	2-4	4-10	1-3		ashes	16AD-18AD	Europe
	Soda Lime	low Al, high Mg	8-20	0-3	3-10	2-10		Plant ashes	>15BC-8BC	Near East
		low Al, low Mg	13-20	0-1	5-10	0-1		Natron	>8BC-3AD	Roman Levant (no Sb_2O_3)
		Low Al,low Mg, High Sb	15-20	0-1	4-6	0-1		Natron	1AD-3AD	Mediterranean area
		High Fe-Mg	16-20	0-1	5-10	1-2		Natron	3AD-5AD	Mediterranean area, Europe
		Levantine glass	10-15	0-1	8-12	0-1		Natron	5AD-8AD	
		High Mg early Islamic glass	10-18	1-3	6-12	3-7		Natron & Plant ashes	9AD-10AD	Islamic world
		Modern	10-20	0-1	10-20	0-1		Synthetic soda	19AD ->	Worldwide
K	potash	Low Mg High K	0-8	8-18	0-4	0-1		Plant ashes	Bronze Age	Europe
		high Al							>1BC	Vietnam, South China
		medium Al								South Asia
		High K European	0-8	8-18	6-20	0-5		Plant ashes	>8 AD	West Europe

		Glass								
		High Lime low Alkali	<10	<12	15-20	0-1		Plant ashes (oak)	15AD-17AD	Northern Europe
Na-K	Mixed	Mixed Alkali Glass	5-10	5-10	10	2-6		Plant ashes (seaweed)	16-17	Northern Europe
Pb	Lead	high Ba							>3BC	China
		high Na							>1AD	China
		High Na							>2BC	Roman
		High-Lead Islamic Glass	8-10	0-2	4-5	0-1	30-40	Natron & Plant ashes	10-14AD	Islamic world
		High-Lead Medieval Glass	0-1	3-10	4-16	1-3	20-65	Plant ashes	8-14AD	Europe

From ~5th BC to ~8th century AD, soda-lime glass, typical Roman glass, were produced in the Mediterranean area using natron, a mineral sodium carbonate-rich (trona) deposit collected from the Levant/Near-East salt lakes [46,48-51]. Low potassium, magnesium and phosphorus levels are characteristic of this glass (Table 1). The sands of River Belus, between Haifa and Acre in present Israel, have been widely cited since Pliny, as the most important sources. Pliny already recognised the interest of shells, a calcium-rich material, presents in the sand. Venetian glaziers used high purity silica such as quartz, chert/flint pebbles which led to the optical quality of *cristallo* and *Façon de Venise* artifacts. Different sub-types are recognised from their minor elements and variation in impurities (Table 1).

From ~8th century to the Middle-Ages in the Mediterranean world, halophytic plant ashes replace natron as a flux and consequently potassium, magnesium and phosphorus levels are larger in glasses produced. However, glass recycling is very common which results in intermediate compositions. In Western Europe, continental plant ashes (beech, oak, bracken but also seaweed) rich in potassium were used to produce “forest” glass to be replaced by imported Spanish Alicante soda ashes (also produced in Sicily, South of France and Carthage). The use of potash-rich fluxes continued till the 19th century. In England, kelp ash was used as the source of potash flux. By end of the 18th century, industrial soda is used, first produced with the Leblanc’ method, thereafter the Solvay process (>1861) [52-54]. As a consequence of the introduction of the Solvay process, glass manufactured after 1861 is characterized by high quantities of sodium and low impurities.

Coloured glasses are more or less easily achieved thanks to different colouring agents [55-59]. In primitive glass production, colour was due to impurities coming from raw materials, mainly iron ions, but very early glaziers tried to control the colour. The 'visible' colour arises from the wavelengths detected by human vision that have not been absorbed by the material. The wavelength absorption is due to (partially empty) electronic levels of some ions (so called "chromophore"), namely the transition metal ions (3d level) and lanthanides/rare earth ions (4f level). Dissolved in the glassy silicate matrix $Fe^{2/3+}$, Cu^{2+}, Co^{2+}, Cr^{3+}, $Mn^{2/3/5+}$, …UO_2^{2+}, Pr^{2+}, … ions colour the glass directly [60]. Alternatively, a phase hosting the above ions, prepared before (pigment) and dispersed in the glass precursor ("*corpo"* and "*anima*" mixing) or formed on cooling by precipitation can colour the glass.

Table 2 Main opacifying and colouring agents

Colour	Elements	Phase	Raman detected	Period	Remarks
White		bubbles	yes		
	Si	quartz (SiO_2)	yes		
	Ti	rutile,anatase (TiO_2)	yes		
	Zr	zircon ($ZrSiO_4$),zirconia (ZrO_2)	yes	>20th	
	P	apatite ($Ca_3(PO_4)_2$)	yes	Antiquity	bones
	Ca	calcite ($CaCO_3$)	yes	Antiquity	
	Sb	antimonate ($CaSb_2O_7$)	yes		
	Sb	antimonate ($CaSb_2O_6$)	yes		
	Sn	cassiterite (SnO_2)	yes	>5AD	
	As	Arsenate $(Ca,Pb)_{1.5}AsO_4$	yes	>17th, >18th	
Blue	Cu	Egyptian blue ($CaCuSi_4O_{10}$)	yes	>3000BC	
	Ba,Cu	Han blue ($BaCuSi_4O_{10}$)	yes	>500BC	
	Ba,Cu	Han violet ($BaCuSi_2O_6$)	yes	>200BC	
	Cu	dissolved Cu^{2+}	no		turquoise in alkali glass matrix
	S	Lazurite ($Na_8[Al_6Si_6O_{24}]S_n$)	yes	>1BC	
		ultramarine	yes	>19th	
	Co	dissolved Co^{2+}	Indirectly		
		spinels $(Co,Cr,X)AlO_4$	yes		

		olivine ($CoSiO_2$)	yes	>17th	
		Co oxide (Co_3O_4)			
	V	zircon (V:$ZrSiO_4$)	yes		
Yellow	Fe	Dissolved Fe^{3+}	no		
	Sb	Pyrochlore ($PbSb_{2-x}M_xO_{7-d}$)	yes	>1000BC	Naples yellow
	Sn	$Pb_2Sn_{1-y}M_yO_4$	yes	Antiquity	
	U	Dissolved UO^{2+}			
	Pb	PbO		Antiquity	
	Sn	Sphene ($CaSnSiO_5$)			Malayite
	Zn,Cr	$ZnCrO_4$		>1800	
Green	Cu	Cu^{2+} dissolved	no	Neolithic	
	Cr	Cr^{3+} dissolved	no		
	Cr	Cr_2O_3	yes	1800s	
		3CaO Cr_2O_3 3SiO_2	yes		Victoria green, Malawyte
	Cr,Co	Spinels:$CoCr_2O_4$,$CoTiO_4$	yes		
		Olivine $NiSiO_4$			
Red	Cu	Cu°	indirect	>Neolithic	
	Fe	Haematite	Yes	15AD	
	Au	Au°	indirect	>16AD	

The power of colouration achieved with pigments is much higher than that obtain by ions. Metal nanoparticles (Cu°, Ag°, Au°) exhibit the highest colouration power [61]. Consequently, different ways are possible to obtain a given colour. For instance, white opacification can be obtained by at least 10 different methods (Table 2): dispersion of (sub) micron bubbles, of (SiO_2) quartz grains, of (SnO_2) cassiterite, of (TiO_2) rutile, of ($ZrSiO_4$) zircon, of lead/calcium arsenate, of calcium phosphate, of calcite, of fluorite, of calcium antimonite particles [56,57]. Blue colour can be obtained with Co^{2+} ions, with lapis lazuli grains, with Egyptian Blue calcium copper silicate and its Chinese barium homologue [62], with cobalt silicate or cobalt aluminate, with cobalt spinel and vanadium-doped zircon. Green colour can be prepared with Cu^{2+} ions or with chromium or nickel-based phases. Alternative technique is the mixing of yellow and blue chromophores [56]. Red colouring agents stable in

a glass matrix are also limited: hematite (Fe_2O_3), hercynite ($FeAl_2O_4$), copper and gold nanoparticles, were the unique colouring agents; - their use was difficult due to their high power of coloration [63] - up to the discovery of the $CdS_{1-x}Se_x$ solid solution. Dispersed as nanoparticles in glass the later mixed compound gives a vivid colouration from yellow to dark red [64].

Thus, the composition of the glass (Table 1) and the nature of the colouring agents (Table 2) can be specific to a period or place(s) of production and hence considered as a *post quem* milestone. However, glass recycling is possible and well demonstrated by the finding of Roman shipwreck cargo made of broken blue glass [49]. Recycling of glass at production workshops led to homogeneous material with composition intermediate between that of the main groups.

We review here the techniques of identification of glass bead technology, provenance and date and applications regarding beads excavated in Africa. The focus on Africa is due to the high number of excavated beads in this continent. For instance, analysis of the bibliography (though not exhaustive) compiled by the Society of Bead Researchers shows 243 works that were published between 1981 and 2016 [65]. The result is summarised in Table 3 based on their locations in Africa.

Table 3 A summary on number of published articles about glass beads found in Africa except Egypt and the east and west coast islands of Africa. Compiled by the Society of Bead Researchers [65]

Location	Country (No. of sites)	Percentage
West Africa	Ghana (13), Mauritania (9), Mali (7), Senegal (3), Burkina Fasso, 2, Niger, Sierra Leone; Benin, 2; Nigeria, 12; Guinea, 1	46%
North central Africa	Congo, 3; Cameroon, 1; Angola, 4	7%
Southern Africa	South Africa, Botswana & Namibia, 17; Zimbabwe, 6	21%
East Africa	Kenya, Uganda and Zanzibar, 12; Ethiopia, 7; Madagascar, 3; Sudan, 5; Tanzania, 2	26%

Bead morphology and classification

Figure 2 shows the variety of size, shape and colour of beads excavated at different archaeological sites in Southern Africa (Botswana, South Africa and Zimbabwe) with occupation dates from ~10th to 19th centuries AD [66-70].

Many scholars attempted to classify the beads as a function of their morphology. The first classification system was proposed by H. C. Beck in 1937 and later refined by L. Malleret in 1949 and by Van Riet Lowe in 1955 [71-73]. New attempts were made by Kidd and Kidd, Van der Sleen and Karklins through the Society of Beads Researchers and others [45-74-76]. The first goal of these morphological classifications was the establishment of criteria that precisely described the shape and colour of the artefacts [77], regardless of the materials and technology used to produce them.

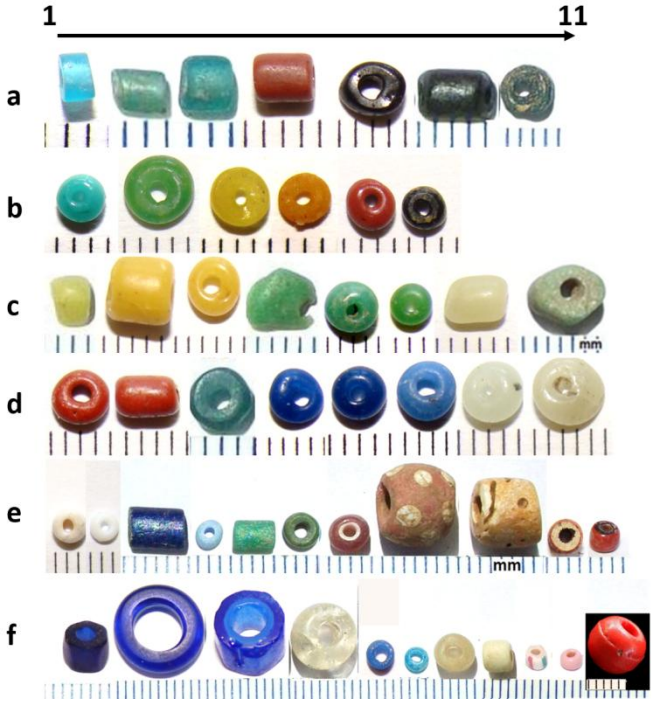

Fig. 2 Bead selection illustrating the variety of shape (tube, cylinder, oblate, minute, mold (e10), etc.) and colour. a) K2-IP series (1-3). (1) turquoise blue, tube (Mutamba), (2-3) blue-green, tube (Basinghall). EC-IP series (4-7). (4) brownish red, tube (5) black, cylinder (Mutamba), (6) black, tube (Basinghall), (7) cobalt blue with Malayite, oblate, wound (Magoro Hill); b) Mapungubwe Oblate (1-6) (Mutamba); c) Khami-IP series (1-7). (1) light green, cylinder (Basinghall), (2-3) yellow, cylinder, oblate (Baranda), (4) green (Basinghall), (5-6) green, oblate (Baranda), (7) white, tube (Baranda), (8) green recycled glass bead, tube (Basinghall); d) Khami-IP series (1-8). (1-2) brownish red, oblate, tube (Baranda), (3) light blue, cylinder (Basinghall), (4-6) cobalt blue, oblate (Baranda), (7-8) white, oblate, cylinder (Baranda); e) European beads with lead arsenate in composition (1-9). (1-2) white, oblate (Baranda). (3-9) found at Magoro Hill. (3) coblat blue, tube (4) light blue, oblate (5-6) green, tube, cylinder (7) white heart, oblate (8) compound bead, sphere, (9) brick red, cylinder. European Soda-rich plant ash (10-11), (10) brownish red on gray (Parma), (11) green heart (Mapungubwe).; f) European beads (1-9). 1) high potash and low phosphate glass, simple-small hexagonal (K2), 2) synthetic soda glass, annular (K2) (3) high potash and phosphate glass, compound-large hexagonal (K2) (4) high alumina soda glass with Levantine ash, un-coloured, sphere (Magoro Hill), (5) coblat blue with calcium antimoniate as opacifier, cylinder (Mutamba), (6) light blue, oblate (Magoro Hill), (7) white, cylinder (Magoro Hill), (8) white. cylinder, (Magoro Hill), (9-10) lead arsenate glass, striped (Mapungubwe), 10) pink, oblate, 11) Red (Zn,Cd)S_xSe_{x-1}, sphere, moulded.

More recently in the Digital Archeological Archive of Comparative Slavery [78] Christopher Decorse [79], drawing primarily on data obtained from excavations at Elmina, Ghana, discusses the potential to use beads as temporal markers in West African archaeology. At the same time, Saitowitz [8] reviewed the classification terms used to describe beads by North American bead researchers and suggests that these could be used in future South African bead studies (see also [80,81]. Wood developed this approach on glass beads excavated from different sites of the 8th-16th centuries in South Africa, for which reliable radiocarbon dates are available [82-84]. Cooperation with Robertshaw's group for the compositional study of glass beads, e.g. those excavated from Chibuene, a 6th-17th century port in southern Mozambique, allows linking morphological and chemical classifications [85,86]. The composition and colour of trade glass beads from West Central of Africa were studied by Rousaki et al. [87] and Coccato et al. [88]. Recently, a review about glass/glass bead local industry in Nigeria has been published [89]. Table 4 lists places where local production has been identified.

Table 4 Identified/expected local production of glass beads

Type	Place	Date	Remarks	References
Garden Roller	K2 Limpopo Valley, SA	K2 (1100-1220)	Molds found with beads. Big beads are made by sintering/melting smaller ones	[85,114,136,137]
Kiffa beads	Kiffa, Mauritania	19th c.	Made from glass powder	[138-140]
Bodom	Ghana Western Africa	19th c.	Powder-glass	[5,141]
Iyun, Segi	Ife, Nigeria	12th-14th c. 18th c.	Grinding, Powder-glass beads	[152]
	Ile-Ife, Nigeria	11th-15th c.	Glass cake, melting beads, high lime-high alumina, high lime-low alumina, soda-lime.	[142]
	Igbo Olokun, Nigeria	11th-15th c.	Crucible production of High lime-high alumina & low lime-high alumina glass from raw local materials.	[89]
Light green drawn bead	Basinghall (Botswana)	1592-1648	Inhomogeneous glass made by sintering soda, mixed alkali and potash glass.	[66]
Blue beads	Carthage/Utica	1st	Grains + glassy cement	[109]

Analytical methods of glass matrix and colouring agents

Recently, Janssens [9] compiled a review of all the techniques for analyzing glass as previously made by, e.g. Pollard and Heron [90]. It is, however, sometimes difficult to apply all the techniques above mentioned on glass beads because of their size and the limited possibilities of sampling. However, the number of beads found on site can be very variable from a few items to more than 100 000, as is the case with Mapungubwe [91]. Analytical techniques of bead analysis have been recently reviewed by Bonneau et al. [6,92]. The most commonly used techniques to analyse glass beads are optical microscopy (OM), scanning electron microscopy (SEM) and associated composition/structure measurement techniques (Energy Dispersive Spectroscopy), X-ray fluorescence (XRF), neutron activation analysis (NAA), laser ablation inductively coupled plasma mass spectrometry (LA-ICP-MS), and Raman microspectroscopy [93]. Three of these methods are non-destructive, non-invasive and can be conducted with portable instruments: OM, pXRF and Raman microspectroscopy [94].

Macro- and microscopic optical observation can answer many questions regarding manufacturing techniques and use of the artefacts [95]. As noted by Bonneau et al. [92] bubbles and striations on the surface of drawn beads are elongated, while those in wound beads tend to be round. Wound beads also exhibit wind marks that encircle the diameter. In the case of blown beads, the presence of elongated bubbles reveals that they were blown in heated drawn tubes rather than free blown. An examination of the ends of a bead may reveal battering suggesting their use in necklaces or bracelets. Finally, microscopic observation reveals the state of degradation of the glass. Optical microscopy magnification is limited to x2000. The diffraction limits the optical resolution to ~0.3 µm.

The magnification of Scanning Electron Microscopes (SEM) is in order of magnitude much higher and allows better the examination of tool traces and the study of secondary phases that are evidence of the raw materials and the technology of production. However, cutting a slice off the beads is generally required to get a representative view: backscattered electron images are very useful to examine the glass heterogeneity, many beads being made not of homogeneous glass but of glass-ceramics, a mixture of glass and micro/nanocrystalline

phases [66,96]. Raman microscopy with high magnification objectives is a non-invasive technique to detect glass heterogeneity at the (sub)micron scale. A great advantage of SEM examination is the possibility to couple the instrument to an X-ray energy dispersive spectrometer (called SEM-EDX or SEM-EDS) at the desired scale. The probed area can vary between a few nm^2 to hundreds μm^2 and the elemental composition, with a rather good accuracy if glass standards are used to validate the procedure can be achieved [96-98]. The small size of most of the beads makes it possible to examine them without special preparation except a good cleaning. However, the important heterogeneity of many glass beads should be taken into account and only the examination of a flat or convex section, instead of a rough surface, provides reliable data. Minor elements are measured as well as traces. Error is usually close to 5-20%, in many cases, less than the heterogeneity of the matter.

X-ray fluorescence (XRF) is very similar to SEM-EDS but the probed area is much larger (hundreds of μm^2 to mm^2) and depends on the instrument and the distance between the instrument and the artefact. Sometimes a camera allows controlling/selecting the analysed area [99]. In this process, X-rays are focused on the sample which is excited and generates new X-rays which characterize the chemical elements. The results are expressed as spectra, as for the SEM-EDS and appropriate calculation lead to the composition, according to some assumptions. Standard laboratory (fixed) instruments can detect elements from carbon to, theoretically, the end of the periodic table, and the X-ray beam goes deeper into the sample (ca. 1μm for SEM-EDS; ca. 10-100 μm for XRF depending of the composition). As for SEM-EDS, the limits of detection (LOD) depend on the chemical elements. To simplify, the typical LOD is about 0.1-2% oxide weight for light elements and about 1 to 25 ppm oxide weight for the heavy elements. Many traces are thus easily measured. As in the case of SEM-EDS, XRF analysis cannot be really quantitative without a ‘plane’ surface and the comparison with glass standards with composition similar to that of the studied material.

The first problem with portable XRF instruments is that elements lighter than magnesium are not measured. Calculation and comparison with references can solve the problem [68,70]. The second problem with the non-destructive XRF analyses with portable instruments on unprepared samples is the lack of plane surface and the difficulty to minimise and keep constant the distance between the artefact and the instrument. X-rays are absorbed/scattered by air and when the control of the artefact-instrument distance is not possible, data should be normalised, using for instance the signal of Silicon (common to most of the phases) or that

intrinsic to the cathode of the instrument (Ag, Rh, etc.). A vacuum pump or helium gas injection eliminates most of the air and increases the reliability of the measurements but decreases the portability of the set-up. The comparison of the signal intensities of elements to find about raw materials and the production technology is often more efficient than the comparison of elemental concentrations, provided by the instrument software.

XRF and EDS analyses are thus very useful in quantifying chemical elements in glass, even in small proportions, and to define glass sub-groups which may be linked to production sites. For provenance studies based on traces, however, the techniques are sometimes not precise enough and neutron activation analysis (NAA) or laser ablation inductively coupled plasma mass spectrometry (LA-ICP-MS) may be better suited for this purpose, if the artefact is sufficiently homogeneous! In particular, last generation of LA-ICP-MS instruments measures isotopes. For instance, lead isotopes can trace mining sources. The method is generally used for finding the source of potteries [17,100].

However, the development of the NAA techniques in the 1960s was at the origin of the impetus of archaeometric and provenance studies [93]. A sample exposed to neutron beam is turned into radioactive isotopes representing the chemical elements present in it. When they return to their stable state, they release gamma-rays which, when recorded using gamma spectrometer, can be related to an atom. As for SEM-EDS and XRF, each level of gamma-ray energy characterizes a specific element in the periodic table. As for XRF, it requires standards for quantitative measurements of elements. One of the great advantages of NAA is that no sampling is generally required for small artefacts like beads. On the other hand, if the artefact is composite like glass ceramics, the results will only reflect the mean composition. Unfortunately, the number of nuclear reactors offering NAA facilities strongly decreased in the last decades and the technique whatever its interest, is now rarely used. Furthermore, the induced radioactivity can dictate that the sample be kept months to years before it can be considered as non-radioactive.

For about 20 years now, Laser Ablation Inductively Coupled Plasma Mass Spectrometry (LA-ICP-MS) replaced NAA to produce accurate mean composition of many materials [34,101,102]. A small part of the material, a ~100 µm diameter spot, is volatilized by a laser pulse, ionised and a mass spectrometer separates and quantifies the atoms (and isotopes for advanced instruments) [100,103]. In many cases for accurate results, the technique requires

knowing the amount of one of the chemical elements in the sample (an “internal standard”, e.g. silicon) before it is analysed. It is a surface technique so testing points need to be free of corrosion. A quick, initial laser ablation of the spot or the line to be tested is often carried out to remove the surface of the samples. The potential measurement of the isotopes offers new tools for provenance identification. The limit of detection (LOD) is very low for many elements and thus the composition of the volatilized matter is determined with high accuracy. However, the representativeness of the measurement can be questioned for many materials and whatever their low sensitivity, data collected by XRF and EDS in combination with imaging techniques offer a more representative view of the material and makes it possible to document and compare better their technology of preparation and origin.

LIBS (Laser Induced Breakdown Spectroscopy) also involves volatilisation of a small volume of material in order to reach the non-corroded material but the elemental composition is determined from the emission spectroscopy [104,105]. The development of this portable technique is recent and has not been used for beads [106].

Raman spectroscopy is another analytical technique, which has been recently applied to glass artefacts. The technique is rather old (1928) but really used in solid state physics since the availability of lasers (>1970) [107]. The so called Raman effect arises from the interaction of a laser beam, i.e. a monochromatic coherent light, with the electron cloud of the chemical bond continuously distorted by the atomic vibrations, or the variation of the chemical bond polarisability. The scattered Raman spectrum forms a set of different peaks; the peak wavenumber position mainly depends on the atom mass and on the interatomic bond force, the peak number and polarisation depend on the symmetry of the chemical bond arrangement (the structure) and their intensity of the local charge transfer (in reference to the conductivity at the very high frequency THz). The information provided is thus very rich. However, the signal is very small and the use of technique remained very limited due to the high cost of the first laser before 2000s.

The first application of the technique to the study of ancient artefacts and of glass started with the availability of the first Raman microscope in 1975 [108]. Due to the very specific interaction of the laser excitation with electronic levels at the origin of the colour (pre-Resonance and Resonance Raman Effects) the sensitivity of the technique is exceptional for the detection and identification of certain colouring agents. Because the Raman effect probes

the chemical bond itself, the technique is also very useful to analyse amorphous and disordered matter. Recent developments in the modelling of the Raman signature of glassy silicates [109-112] as well as the increased sensitivity and miniaturisation of the instruments led to a rapid development of its use in many areas [94].

Briefly, the Raman spectrum of a glassy silicate is composed of two massifs (broad peaks): one centred at ca. 500 cm^{-1} (SiO_4 tetrahedron bending modes) and the other at ca. 1000 cm^{-1} (SiO_4 tetrahedron symmetrical stretching modes), of a broad "Rayleigh" wing, and of the so-called Boson peak arising from the contribution of librational and lattice modes below 300 cm^{-1}. The contribution of other modes is not significant in a first approximation. Calculating the area under each two massifs and dividing them reveals the polymerization index ($Ip = A_{500}/A_{1000}$) which is related to the glass nanostructure and thus related to the processing temperature of the glass [109].

The Raman spectrum constitutes a fingerprint of the glass composition and structure. The stretching massif can be investigated using the "Q_n model" which depends on the relative proportion of the different SiO_4 entities constituting the glass: isolated tetrahedron (Q_0) and tetrahedral connected by 1, 2, 3 or 4 common oxygen atoms [112]. Combining the above characteristic parameters make it possible to identify sub-groups of glass types [112,113]. Identification of the glass type (potash, lead-based, high lime-low alkali, soda and soda lime glass) is possible from the visual measurement of the massif maximum wavenumbers (see the next section). Complementary classification of sub groups is possible after considering more complex parameters [111]. So far, only a few studies have to date used Raman spectroscopy on glass beads [66-69,88,92,114-118]. This technique has, however, proven its suitability and significance in other glass studies, especially in the identification of opacifying agents and pigments [18,21,24,60,64].

Thus, with the availability of portable instruments, Raman spectroscopy is an inexpensive and quick technique to obtain information from glass beads. As a scattering method, its great advantage is that no preparation or sampling is required. Different lasers from UV to nIR can be powerful; however, the power of illumination should be adapted as a function of the light-matter interaction [119]. If the material is transparent for the laser wavelength (i.e. no absorption) a few tens $mW/\mu m^2$ is convenient, but if the wavelength is absorbed (pre-

Resonance and Resonance Raman Scattering), 0.1 µW/µm^2 or less can induce a strong local heating and phase transition/oxidation reactions can take place.

Fluorescence, another optical phenomenon much more intense than the Raman spectrum, can overlap with the Raman spectrum, making its exploitation difficult. Actually, the phenomenon is common for excavated materials because of the biological films that form in the soil at the surface and in the cracks of the materials. This film and the associated very broad fluorescence are easily destroyed by illumination by UV and blue laser lines. With green excitation the elimination of the fluorescence is progressive if the power of illumination is not sufficient. Ion beam accelerators and Synchrotron sources also offer good analytical techniques [93] but have not been used for bead studies to date.

Bead type identification

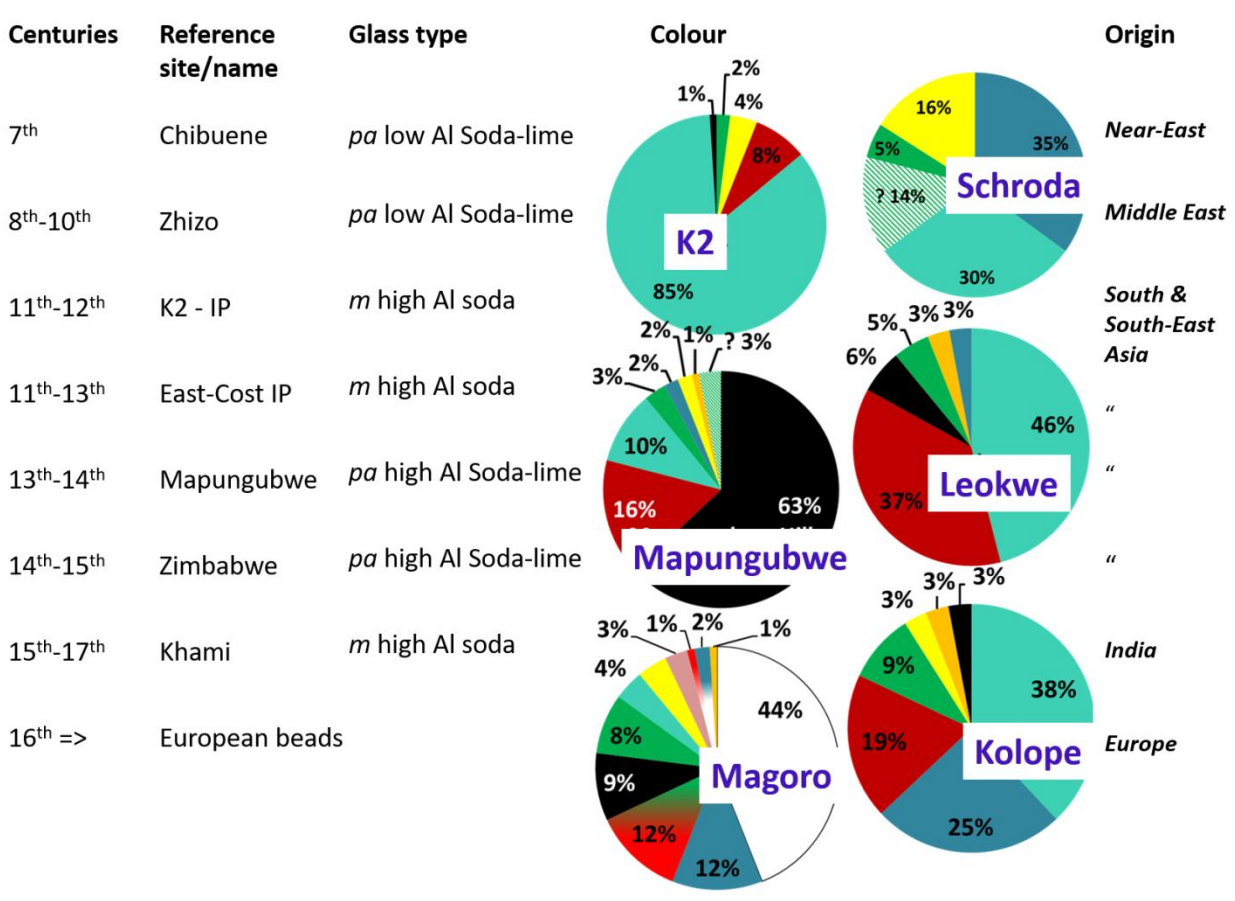

Fig. 3 Schematic of the bead series according Wood' morphological classification [67,82,84]. Corresponding composition type and colour palette are given (see text).

Fig. 4 Map shows the sites referred to in the paper

Figure 3 summarizes Wood' classification: eight series of beads are recognized, named according to the type of site first studied and for which radiocarbon dates are available [82-84] (Figure 4). The great variety of colour set with time is obvious. The oldest series (7th-8th centuries) is linked to Chibuene, an Indian Ocean port located on the African coast of Mozambique, between the Limpopo and Zambezi River mouths. The beads are expected to have been produced in the Middle East. Chibuene series are made of low alumina (Al_2O_3 < 5%) plant ash glass and could be differentiated from the later Zhizo series with lower magnesia (MgO<3%) and higher potash [86]. The second ancient group is called Zhizo, an earlier Iron Age cultural phase that expanded in much of southern Africa between 8th and 10th centuries [120]. The beads arrived in southern Africa through the port of Chibuene as well [84]. Most of these beads are cut from drawn tubes. Figure 3 shows the colour distribution of the beads from the contemporary site of Schroda [82]. These low alumina soda-lime glass beads are blue, turquoise, yellow and rare dark green. They are probably produced in the Near/Middle East [85].

The third group, K2-IP (IP for Indo Pacific), is associated with the famous K2 site, very close to Mapungubwe Hill, in the middle Limpopo River valley, close to the modern borders of South Africa, Zimbabwe and Botswana [91]. K2 beads are also recovered from other regions

(e.g. Mapungubwe and Leokwe) and distant sites in Madagascar and Mozambique with contemporary archaeological context [85,97,121,122]. The colour of this high alumina (mineral) soda glass is mainly turquoise and green (Figure 3). Brownish-red and black beads with the same glass composition belong to the late K2 period and are similar to the beads found in the East Coast of Africa (EC-IP series) [83]. The yellow beads belong to EC-IP series as well but arrived in the region with the K2 turquoise beads [83]. The beads of the mid-10th to 13th centuries period (K2 and EC) with high alumina mineral soda composition are grouped in IP series and assumed to be imported from south and Southeast Asia. The variety of colours in EC-IP is more than the K2-IP series and consists of green, yellow, black and brownish-red.

The next series is called Mapungubwe Oblate and the composition is different, with a higher magnesium content (plant ashes soda lime with high alumina). Note that the Leokwe colour palette (Figure 3) is intermediate between that of K2 and Mapungubwe where ~60 % of the beads are black, the other being brownish-red, turquoise, green, blue and yellow. The last series before the arrival of Portuguese merchants is the so-called Zimbabwe series [84], with similar composition as Mapungubwe.

The latest non-European series is Khami, after the name of a site in Zimbabwe. The composition is different, mineral high alumina soda glass close to preceding IP series. The colour palette is also different, for example the beads from Kolope site (16th century) [82]. The bead colours are turquoise, blue and brownish-red plus rare green, black, yellow and orange. Blue (cobalt) beads of IP series were imported for the first time during the Khami period. This period coincides with the arrival of European traders (first the Portuguese, then Dutch merchants) but the number of European beads is very low as observed at Baranda and Danamombe [69,70]. It is only in the mid-17th century that a rise in European bead numbers and a variety of colours and compositions is documented [67,123]. The colour examples of European beads are that of Magoro Hill, in the Limpopo province of South Africa [67]. It has been demonstrated that many morphological criteria of the Wood classification do not work and may lead to false identifications because European producers copied shapes and colours of ancient beads, highly prized by the African communities [67].

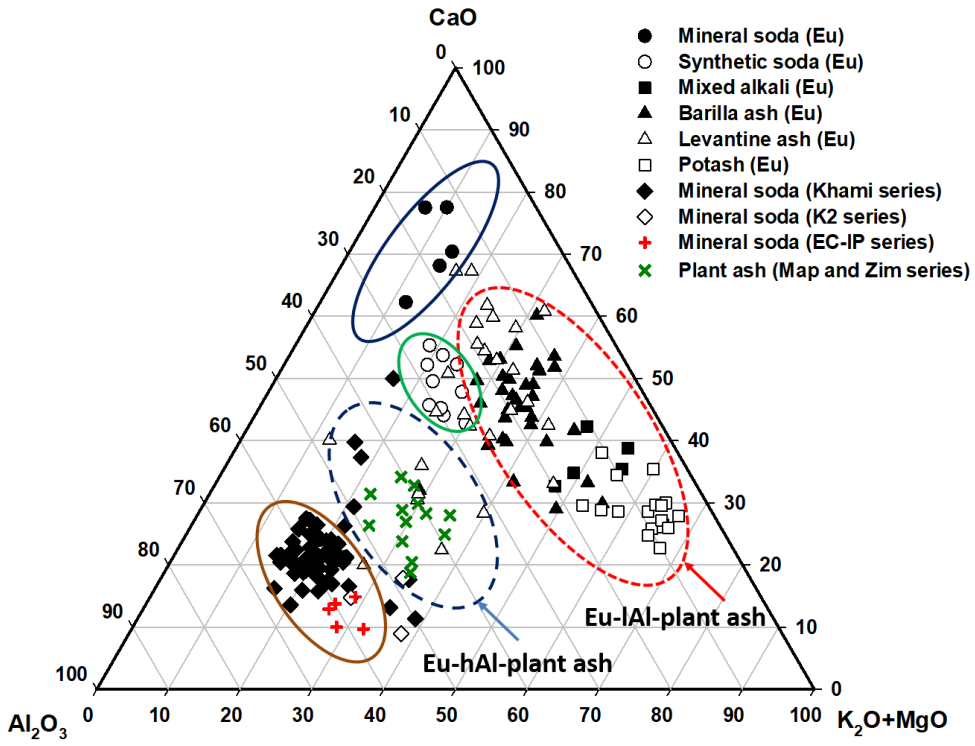

Fig. 5 Al-Ca-Mg+K oxides ratio diagram highlighting the different types of glass (h: high; l: low). The symbols used for each series are given. Dashed lines and solid delimit main soda-lime plant ash glass and soda compositions.

Figure 5 shows the different types of composition located in Al, Ca and Mg+K oxides ternary composition diagram. This type of diagram discriminates very well, i) the high alumina from the low alumina glass (high alumina glasses are recognized as characteristic of South Asian and South Europe productions), ii) the potash from the soda-lime glasses and iii) the mineral from the plant ashes glasses (Mg level). The example is made with the beads excavated at Magoro Hill, an important site related to the Limpopo River trade and occupied almost continuously from the 7th to the 19th century. Other samples belong to Mutamba (13th -14th AD), Maryland and Parma (15th-20th AD) middle and late Iron-Age sites in the north of South Africa and Baranda (16th-17th AD) in Zimbabwe. Six of the above mentioned series are identified. It is also possible to discriminate 6 European glass compositions as follow: soda-rich plant ash glasses of north and south of Europe (15th-18th AD), potash glass of central Europe (early 18th-mid 19th AD), mineral-soda glass (recycled), synthetic-soda glass (19th AD) and mixed alkali glass. The south European glass except Venice productions contains higher alumina (>3%) compared with north and central Europe productions [124].

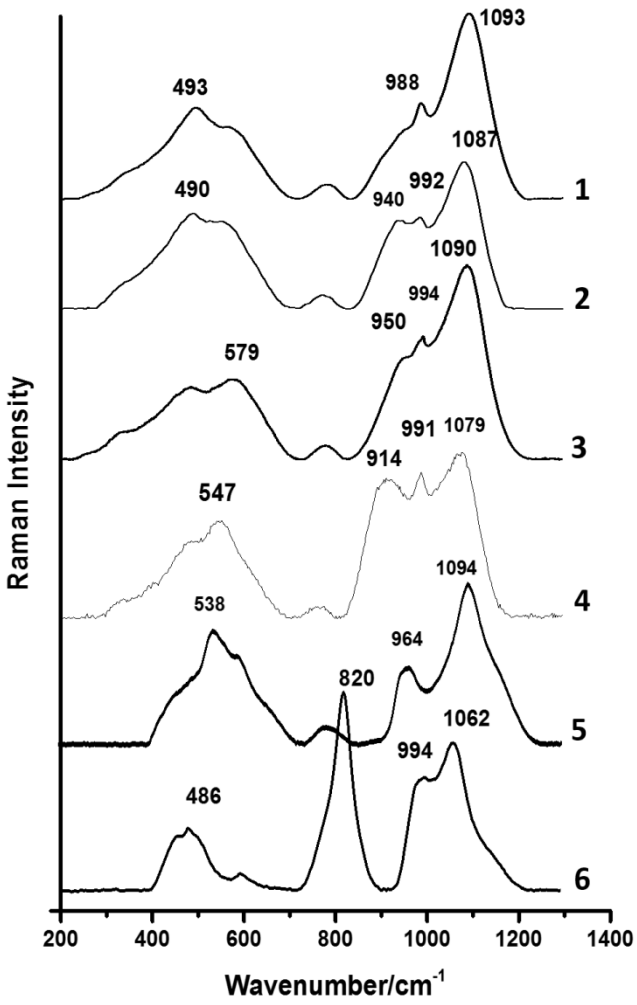

Fig. 6 Representative Raman signatures of: 1) soda glass of IP series; 2) soda glass with high iron content uses as colorant; 3) soda/lime glass of Mapungubwe oblate, some of Khami-IP series and European beads; 4) soda/lime glass with high iron content (mostly recorded for green and yellow Khami-IP series); 5) soda/lime glass, recorded on European beads with high potassium; 6) lead arsenate glass, European beads. A baseline has been subtracted according to the procedure described in Colomban [110].

Figure 6 shows the different types of Raman signatures encountered. The Raman classification of the glass network made from the wavenumber of the summit of the two main Raman peaks, the bending and stretching modes of the SiO_4 tetrahedron, the basic unit of silicate glasses is given in Figure 7. The classification method is somewhat different from that obtained by considering elemental composition, more clear to discriminate soda from soda-lime glass and many European beads than the composition tables [125,126]. Mineral soda glass of IP series and some of European beads is identified with maximum peaks around 450-510 cm^{-1} and 1100-1060 cm^{-1} (Figure 6, spectra 1 and 2) [116]. Colorants and impurities in glass effect on the shape of spectrum, as it observes in Spectrum 2. This spectrum belongs to EC and Khami-IP beads with high iron, used as colorant in combination with copper to form red, green and blue-green beads [66].

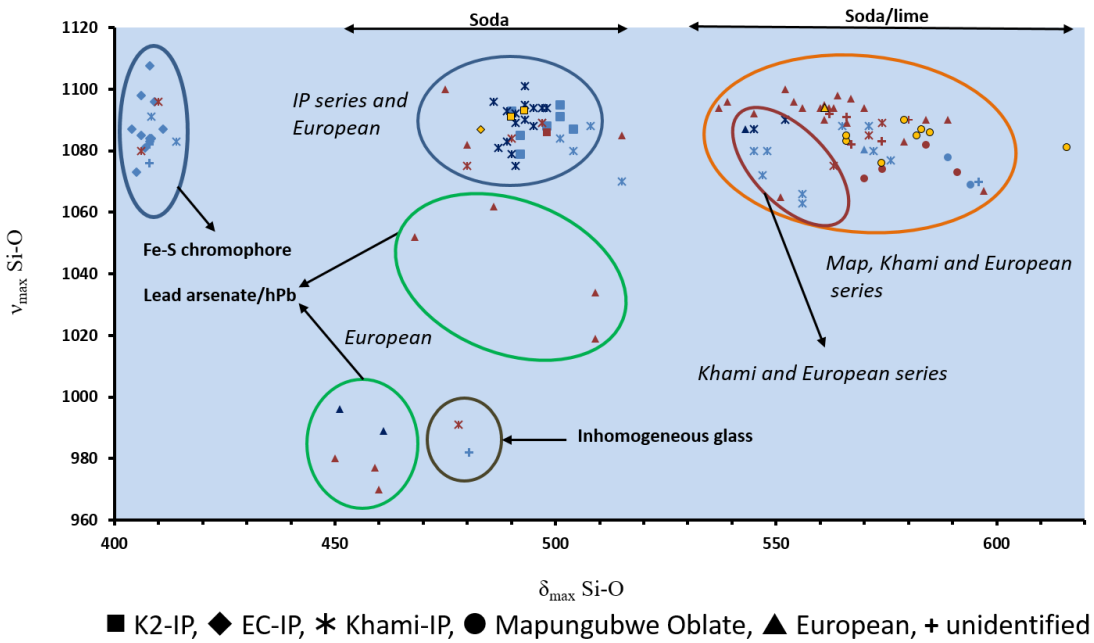

Fig. 7 The plot of Si-O bending vs stretching vibration of glass beads found at southern Africa, classifying the different glass series. Basinghall Farm (light blue), Baranda Farm (dark blue), Magoro Hill (brownish-red) and Mutamba (yellow).

All Mapungubwe, Zimbabwe series, some of Khami and European series show a shift in bending massif toward a higher wavenumber (550-620 cm^{-1}), the characteristic of soda-lime glass (Figure 6, spectra 3 and 4) [109]. Spectrum 4 was recorded on EC and Khami-IP beads with high iron content [66]. Spectra 5 and 6 belong to European beads (Bohemian hexagonal beads) with high potassium (potash-lime) and lead arsenate glass respectively [67]. The maximum peak in SiO_4 stretching component shifted downward (<1060 cm^{-1}) in lead-based glass and its bending summit is around (450-500 cm^{-1}) that made a cluster beneath the soda group (Figure 7). The same shift is observed for the beads with high calcium content and inhomogeneous chemical structure (recycled glass) (Figure 8, spectrum 9). This identification can be made by field archaeologists with the portable instrument on site.

Matrix and colouring agent composition as chrono-technological markers

Table 2 lists the different opacifying and colouring agents of glassy silicates observed in our beads studies [56]. As mentioned above, the first glasses have a green hue due to impurities, mainly iron ions. Later, with finding the capacity of manganese ions in absorption of visible light formed by Fe^{3+} ions, the green hue was eliminated. Copper which gives turquoise (Cu^{2+} ion in an alkali glass), green (Cu^{2+} in lead glass) or red (Cu° nanoparticles in (lead) glass) was used since Neolithic times [61].

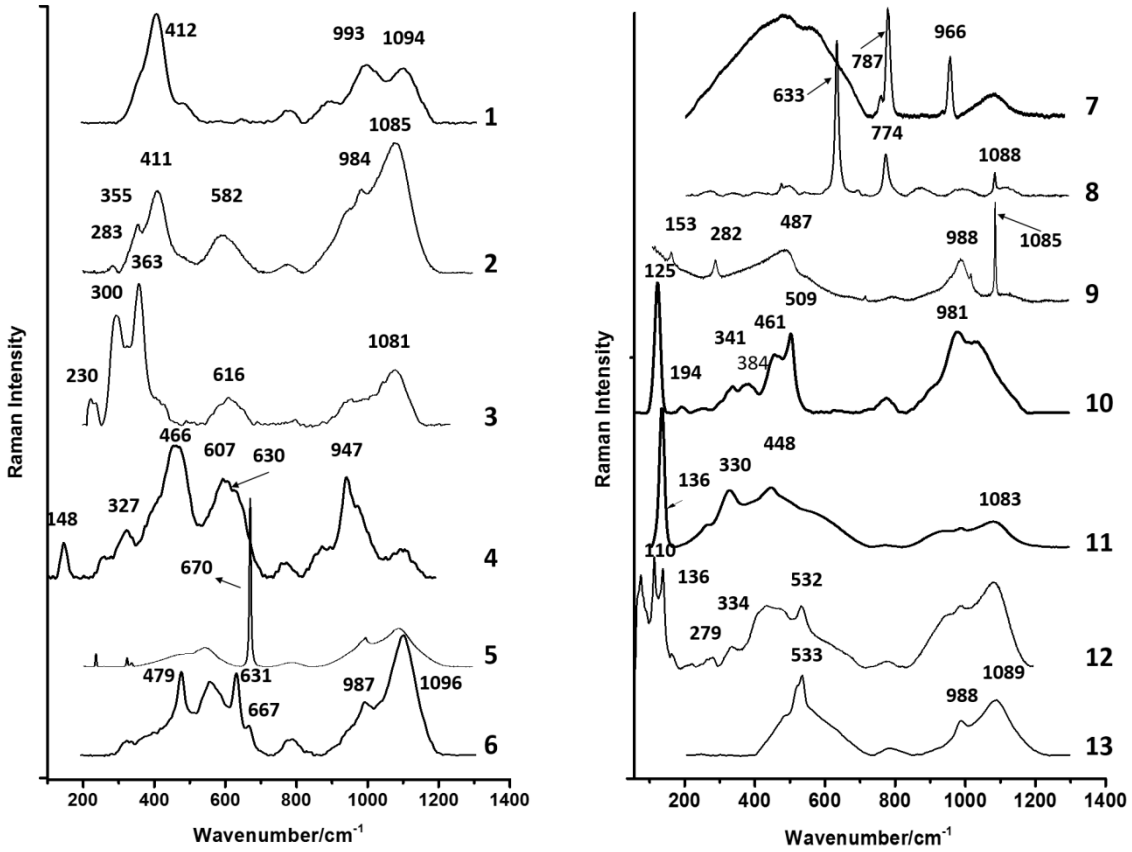

Fig. 8 Representative Raman signatures of pigments, opacifiers and secondary phases: 1) Fe-S chromophore in black IP series; 2) Fe-S chromophore with an extra peak at 355 cm^{-1} that shows a high concentration of the chromophore (IP series); 3) Fe-S chromophore in black Mapungubwe Oblate. (Mutamba); 4) Manganese oxide (Jacobsite) in black European bead (Magoro Hill); 5) calcium antimonitae ($CaSb_2O_6$) used as white pigment in a white European beads (Baranda); 6) calcium antimonitae ($CaSb_2O_7$ and $CaSb_2O_6$) in one European beads (Magoro Hill); 7) Malayite in one cobalt blue bead (Magoro Hill); 8) Tin oxide used as opacfier in Mapungubwe Oblate (Mutamba); 10) calcium carbonate impurity in a recycled glass bead (Basinghall); 11) Pb-Sn-Sb triple oxide in European beads (Magoro Hill); 12) Lead tin yellow (II) detected in Khami-IP and Mapungubwe series; 13) a mix of lead tin yellow (II) and lead oxide in orange Mapungubwe oblate and Khami-IP; 14) Lazurite in blue European beads (Magoro Hill).

Calcium antimonates were used in Mesopotamia very early to opacify glass. Cassiterite was used at the end of Roman times as opacifier [96] before being largely used by Islamic craftsmen [127,128]. Antimony and tin are major impurities of lead oxide, the main flux of many glass and glazes, therefore, their precipitations in lead-based glass and glazes were not really controlled at the beginning. Consequently, improved technologies were lost repeatedly. In the same order, cobalt was used episodically by the Egyptians of the 18th Dynasty (~1500 B.C.) to colour glass, and then stopped for centuries [56]. Bonneau et al. [92] established

quantitatively the transition between the use of SnO_2 (1590-1699), Sb_2O_3 (1590-1900) and "$PbAsO_4$" (1799->1900) as white opacifiers with the study of beads traded in North America.

Lapis lazuli was used by Ptolemaic glassmakers [18], then by some Roman ones [19] and then unobserved for centuries up to its extensive use at Normand Court [20] and then during the Mamluks Dynasty [21]. Egyptian blue continued to be used by Roman glaziers and potters before its disappearance [129]. At about the same period Han glass was coloured with the barium homologue of Egyptian blue [62,130,131].

Green shades remained for a long time difficult to prepare: Cu^{2+} in lead-based glass was the only method, turquoise being obtained when in lead-free glasses. With the limited coloration power of dissolved transition metals in the glass network, an alternative way was the mixing of yellow with blue colour, e.g. the dispersion of a yellow pigment (lead oxide, Naples yellow pyrochlore or lead-tin homologue, (see below) in a glass coloured in blue with Co^{2+} ion or/and lapis lazuli grains forms green colour [21].

Red colour was also rather difficult to obtain: copper nonoparticles have a very high power of coloration and their amount should be limited to obtain a vivid colour. The dispersion and the grain size of hematite should also be very controlled to obtain vivid red or orange. Highly vivid red to yellow colour is obtained with $Cd_{1-x}S$ nanoparticles from the first quarter of 20th century up to ~1980 [64,115]. As demonstrated in the above mentioned examples and those given in Table 2, more or less similar colours are obtained with a large variety of colouring agents that well characterise the production made in a given place and period.

Figure 8 shows typical Raman signatures of pigments observed on glass beads from Southern Africa sites of Mapungubwe, K2 [116,118], Basinghall [66], Magoro Hill [67], Mutamba [68], and Baranda [69]. The spectrum recorded on black beads shows the strong ca. 300-400 band characteristic of Fe-S resonance Raman modes of the amber chromophore (spectra 1-3) [114]. The quantity of black beads increased with the arrival of Mapungubwe oblates (Figure 3). Although both series of black (IP and Mapungubwe) were coloured with Fe-S chromophore, earlier series (IP) contain a more homogenous spinel pigment with consistent Raman spectrum (spectra 1-2). The Fe-S chromophore in Mapungubwe series has a complex structure as recorded spectra show (spectrum 3), a criterion that is used for discrimination of black of two series with the same shape.

Spectrum 5 shows the characteristic signature of Sb_2O_6 antimonite (670 cm^{-1}). Spectra 6 and 8 show respectively Sb_2O_7 antimonite (479-631 cm^{-1}) and the cassiterite SnO_2 (633-774 cm^{-1}) doublets of the main opacifyers. Cassiterite as an opacifier is limited to green and turquoise beads of Mapungubwe oblate among the pre-European series. The 136, 330 and 448 cm^{-1} triplets (spectrum 11) are characteristic of Naples Yellow Lead-tin (II) pyrochlore and additional 110 cm^{-1} (spectrum 12) indicates a saturation with lead oxide [132-134]. The yellow pigments are widely used in the yellow, orange and green beads of Mapungubwe, Khami and European series.

Spectra with calcite signature (Basinghall) at 1085 cm^{-1} (spectrum 9) are observed in beads made from recycled glass and probably a local production. Undissolved calcite phase remained in the glass matrix due to the low melting temperature or the short duration of melting process, according to a production far away from main glass production centres. Peaks at 285-288 cm^{-1}, chalchopyrite $CuFeS_2$, are observed in IP and Mapungubwe black and inhomogeneous green beads (spectra 2 and 9).

Specific secondary phases with characteristic Raman signature offer a method to identify specific production. For instance, the chrome-doped malayite, a synthetic sphene, a phase used as pink pigment since the 18th century [135], was detected in some of Indo-Pacific beads (spectrum 7) found in different sites namely, Antsiraka boira, Mayotte (12th-13th century), Magoro, South Africa (13th-17th century) [67,97]. The source of these beads is different from IP series found at K2, Mapungubwe and Mutamba since the phase was not detected in this series. The only bead found in Magoro Hill with malayite is a cobalt blue with a high manganese as impurity that makes the colorant close to cobalt sources of Far East Asia (Figure 2, a7).

Recycled glass and/or heterogeneous bead

Figure 9 shows the element map of a bead section: an example of a bead made by recycling ancient glass pieces with very different composition, sodium and potassium-based respectively [66]. SEM-EDX mapping is very didactic but the same information can be obtained by Raman scattering, non-destructively, by collecting the Raman spectrum in different spots, the size of the analysed surface being chosen from a few μm^2 to a few tens/hundreds of μm^2. At K2 (1100-1220 AD), the local preparation of big beads (the so

called Garden Roller) by sintering/melting together small beads in a clay mould is well documented [114,136,137]. Local productions are also documented in other region of Africa (Table 4), for instance, Carey [138], Opper and Opper [139] and Simak [140] report that such beads have been produced at Kiffa in southern Mauritania. Haigh [141] and Francis [5] report the modern production of "powdered-glass" or "*bodom*" beads in a number of villages in south-central Ghana.

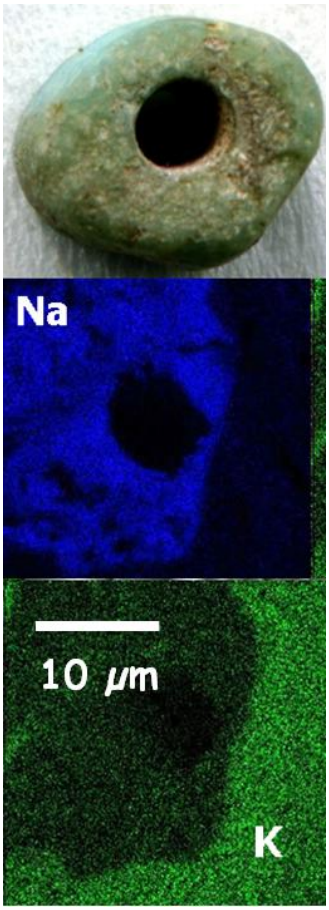

Fig. 9 Example of recycled bead (local production): SEM-EDX element mapping highlights the mixture of soda- and potash-glass grains.

The composition of glass beads from Southwest Nigeria (Ile-Ife), determined by LA-ICP-MS, shows unusual high lime - high alumina (HLHA) contents [89,142]. The simultaneously high content of the lime and alumina in Ile-Ife glass does not match with the database of glass compositions of the Middle East, Roman, ancient Islamic, and Southeast Asia unprecedented. The concentration of these oxides separates the Ife glass from other known compositional groups [143,144]. As a result, Lankton et al. [142] conclude that the HLHA glass is evidence of a glassmaking tradition unique to West Africa, which was locally manufactured in or near Ile-Ife. Recycled glass implies complete melting and homogenisation. This is possible if the craftsmen have the rare skills and furnace to melt and produce glass.

Heterogeneous glass is different from recycled glass. It's a glass made by sintering of glass beads or of crushed glass. One of the glasses (or raw materials added) melts and cements the grains. The skills and tools required are easier and hence beads made of sintered glass are potentially local production. But, local productions can be established only if moulds have been found as at Mapungubwe (12th-13th century, South Africa) and Igbo Olokun (11th-15th century, Nigeria) (Table 4). Comparison of composition or Raman signature recorded in many spots on the same bead or better composition mapping and microstructure imaging are needed to identify a bead made of sintered glass grains. At K2 site, the Garden Roller beads are produced by sintering together minute beads [114,136].

LA-ICP-MS composition studies postulate that the composition measured on a rather small bead region is representative because glass beads are homogeneous. This postulate is wrong in many cases because the heterogeneity due to the use of pigments (the size of pigment grains can reach a few tens microns and their distribution is not homogeneous [96]. On the other hand, pure pigment Raman signatures and glass matrix signature are currently obtained with x10 to x200 objectives that probe a volume variable from ~25x25x100 to 0.5x0.5x3µm^3. Recording Raman spectra in different spots easily detect heterogeneity. SEM or optical images and elemental mapping (Figure 9) are necessary to give a view of the heterogeneity (grains/particulate size, presence of intergranular cement, of different glass composition, etc.) [67]. XRF measurements made with portable instrument, whatever their much lower accuracy by comparison with LA-ICP-MS measurements, gives a mean value. The combination of Raman, XRF and LA-ICP-MS and optical or electronic microscopy is the best procedure to have representative information and to detect beads made of glass mixture.

Discerning between European replicas and earlier, ancient beads

The numbers of potential places of production and trade pathways are less for beads found in earlier sites (<15th century). In the later sites with European archaeological context a combination of old and modern beads with a variety sources are found. Some European beads are imitations of older series consequently morphological classification of beads could not work properly for revealing the link between bead series and some production places. The composition of glass matrix, pigments and opacifiers is essential for discerning European beads from pre-European series. Calcium antimoniates (Figure 8, spectra 5-6), arsenates

(Figure 6, spectrum 6), Pb-Sn-Sb triple oxide (Figure 8, spectrum 10) manganese oxide (Jacobsite) (Figure 8, spectrum 4) in European beads are some of the pigments that were not detected in pre-European series in southern Africa.

The majority of European glass beads included soda-lime plant ash, mixed alkali, potash and mineral soda, and can be discriminated from the earlier trade series (IP, Map and Zim series) with their low percentage of alumina in the composition (Figure 5). Only few numbers of European beads have the same ratios of alumina, lime and potash as the Southeast Asian plant-ash glass beads categorized as Mapungubwe and Zimbabwe series [145]. These European beads which contain high alumina content (>3%) were produced in southern Europe using sand and Levantine or West Mediterranean alkali. These beads can be discriminated from earlier series by secondary phases (pigments or opacifiers) in the glass.

Impurities and secondary phases in glass is also a very useful factor in identifying European beads. Most European beads contain a lower amount of titanium and iron compared to pre-European series. Except for some lead arsenate beads, uranium is very low in most of European beads (<10 ppm). On the other hand, silver and nickel are found as the impurity of cobalt in some of European blue beads and manganese in Asian productions [146-148].

Perspectives

The use of beads as currency and or exchange tools has been reported by some authors [149-151]. It is noteworthy that huge changes of the colour distribution as a function of long period of trade, as exampled in Figures 2 and 3, are observed. The availability of some colours could be limited because the need of special raw materials such as cobalt or lapis lazuli. In that case the origin from special sites of production is likely. Lack of cobalt blue in the earlier IP series (mid-10th - 13th century) as the function of changing the trade route from the Middle-East toward South and South-East Asia is a case [83]. After the demise of the Zhizo series, the K2 turquoise blue was the prominent colour and due to its availability and colour preference of native consumers easily took the place of cobalt blue.

It took time for new colours (brownish-red and black) to be accepted by hinterland inhabitants in southern Africa. It was only after 1020 and the late K2 period that a low number of brownish-red and black IP beads appeared in archaeological context respectively

while yellow and green IP beads (close to Zhizo series colours) found their market at the same time as K2 turquoise blue [83]. On the other hand, the production of turquoise beads (coloured with Cu^{2+} ions) is easy. Accordingly, the proportion of turquoise beads to other colours is generally important. One could assume that the values of these common beads will be lower. The knowledge of the value and equivalence of the different types of beads as a function of time and place should be very interesting to get economic information, as obtained by checking the quantity of slag produced in an iron workshop or the purity of gold in gold artefacts and coins. Colour choice is also cultural parameters that could be changed with the community traditions [77].

Surprisingly, black and brownish-red replaced turquoise blue colour with a significant social economical change in the area and the movement of capital from K2 to Mapungubwe in 1220. This is in coincidence with changes in the pattern of trade, the appearance of a new beads series (Mapungubwe series) and a new demand for the beads. The evidence mentioned above shows the inhabitants did not easily accept a new colour therefore, the change in colour preference of inhabitants might be related to the social and economical changes and the new imported beads colour palette and numbers of each colour in the market.

The big interest in portable instruments such as Raman and XRF set-ups is their operability on site by non-specialists, with a rapid performance in analysing of representative items, selected by experts. This could help to accede to a statistical view of the artefact categories. Recent studies show the efficiency of the techniques in discriminating glass beads categorized as K2, East Coast, Mapungubwe, Khami and European series. Among different beads colours; turquoise blue, green, yellow, red and black because of the same pigmentation pattern in their production would be hard to be discriminated in series with the same glass matrix. It is necessary to gather more information about impurities presents in each series with analysing of more beads from undisturbed and well dated archaeological context. More comprehensive studies are also needed to document local production of glass beads. Microstructure should be considered with attention to detect sintered glass and hence potential local production.

Acknowledgments

Farahnaz Koleini, Linda C. Prinsloo and Innocent Pikirayi acknowledge the financial contribution from the National Research Foundation (NRF) of South Africa with UID grant numbers of 85178, 81857 and 105866.

Authors contribution

All authors contributed to conceptualization, Writing & Editing.

References

1. Poupeau, G.; Le Bourdonnec, F.X.; Carter, T.; Delerue, S.; Shackley, M.S.; Barrat, J.A.; Dubernet, S.; Moretto, P.; Calligaro, T.; Milic, M.; Kobayashi, K. The use of SEM-EDS, PIXE and EDXRF for obsidian provenance studies in the Near East: a case study from Neolithic Çatalhöyük (Central Anatolia). *J. Archaeol. Sci.2010,* 37(11), 2705-2720.

2. Tykot, R.H. Chemical fingerprinting and source tracing of obsidian: The Central Mediterranean trade in black gold. *Account of Chemical Research* 2002, 35 (8), 618-627.

3. Beaujard, Ph. Un seul système-monde avant le 16e siècle? L'océan Indien au cœur de l'intégration de l'hémisphère afro-eurasien. In *Histoire globale, mondialisations et capitalisme ;* Beaujard, Ph., Berger, L., Norel, P., Eds.; La Découverte-Recherches: Paris, 2009; pp. 82-148.

4. Beaujard, Ph. *Les mondes de l'océan Indien, Vol. 1, De la formation de l'État au premier système monde afro-eurasien, Vol. 2. L'océan Indien, au cœur des globalisations de l'Ancien Monde (7e-15e siècles)* ; Armand Colin : Paris, 2012.

5. Francis, P. Jr. *Asia's Maritime Bead Trade, 300BC to the Present*; University of Hawaii Press, 2002.

6. Bonneau, A. ; Moreau, J.F. ; Hancock, R.G.V. ; Karklins, K. Archaeometrical analysis of glass beads : potential, limitations, and results. *Beads: J. Soc. Beads Res.* 2014, 26, http://surface.syr.edu/beads/vol26/iss1/7

7. Hancock, R.G.V.; McKechnie, J.; Aufreiter, S.; Karklins, K.; Kapches, M.; Sempowski, M.; Moreau, J.F.; Kenyon, I. Non-destructive analysis of European cobalt blue glass trade beads. *J. Radioanal. Nucl. Chem.* 2000, 244 (3), 567-573.

8. Saitowitz, S.J. Classification of glass trade beads. *South. Afr. Mus. Bull.* 1988, 18(2), 41-45.

9. Janssens, K. ed. *Modern methods for analysing archaeological and historical glass*, 1st ed.; J. Wiley & Sons: Chichester, 2013.

10. Brill, R.H. The Chemical interpretation of the texts. In *Glass and glassmaking in ancient Mesopotamia*; Oppenheim, L., Brill, R.H., Barag, D., von Saldern, A. Eds.; The Corning Museum of Glass, NY: New York, 1970, pp. 105-108.

11. Henderson, J. *Ancient glasses, an Interdisciplinary exploration*; Cambridge University Press: Cambridge, 2013.

12. Shortland, A.J. *Lapis Lazuli from the kiln: Glass and glassmaking in the Late Bronze Age;* Leuven University Press, 2012.

13. Tite, M.S.; Shortland, A.J. *Production technology of faience and related early vitreous materials*, Monograph 72; University of Oxford: School of Archaeology, Oxford, 2008.

14. Jackson, C.M. Making colourless glass in Roman Period. *Archaeom.* 2005,47(4), 763-780

15. McGray, P. ed. *Prehistory and History of Glassmaking Technology; Ceramics and Civilization Series*, Volume VIII; The American Ceramic Society: Westerville, 1998.

16. Schuler, F. Ancient glassmaking techniques: the molding process, *Archaeol.* 1959, 12, 47-52.

17. Degryse, P., Schneider, J. Pliny the Elder and Sr-Nd isotopes: tracing the provenance of raw materials for Roman glass production. *J. Archaeol. Sci.*2008, 35(7), 1993-2000.

18. Caggiani, M.C.; Colomban, Ph.; Mangone, A.; Valloteau, C.; Cambon, P.) Mobile Raman spectroscopy analysis of ancient enamelled glass masterpieces. *Anal. Methods* 2013, 5, 4345-4354.

19. Greiff, S.; Schuster, J. Technological study of enamelling on Roman glass: the nature of opacyfing, decolourising and fining agents used with the glass beakers from Lübsow (Lubieszewo, Poland). *J. Cult. Herit.*2008, 9 Supplement, e27–e32.

20. Caggiani, M.C.; Valloteau, C.; Colomban, Ph. Inside the glassmaker technology: Search of Raman criteria to discriminate between Emile Gallé and Philippe-Joseph Brocard Enamels and Pigment Signatures. *J. Raman. Spectrosc.*2014,45 (6), 456-464.

21. Colomban, Ph.; Tournié, A.; Caggiani; M.C.; Paris, C. Pigments and enamelling/gilding technology of Mamluk mosque lamps and bottle. *J. Raman. Spectrosc.* 2012, 43(12), 1975-1984.

22. Henderson, J. Tradition and experiment in first millennium A.D. glass production. The emergence of early Islamic glass technology in late antiquity. *Acc. Chem. Res.* 2002, 35(8), 594-602.

23. Davidson, S.; Newton, R.G. *Conservation and restoration of glass*; Routledge, 2008.

24. Ricciardi, P.; Colomban, Ph.; Tournié, A.; Milande, V. Non-destructive on-site identification of ancient glasses: genuine artefacts, embellished pieces or forgeries? *J. Raman. Spectrosc.*2009, 40, 604-617.

25. Cothren, M.W. *Picturing the celestial city: The medieval stained glass of Beauvais Cathedral*; Princeton University Press: New Jersey, 2006.

26. Cummings, K. *A history of glass forming*; University of Pennsylvania Press, 2002.

27. Sayre, E.V.; Smith, R.W. Compositional categories of ancient glass. *Science* 1961, 133(3467), 1824-1826.

28. Galuska, L.; Machacek, J.; Pieta, K.; Sedlackova, H. The glass of great Moravia: Vessel and Window glass, and small Objects. *J. Glass Stud.* 2012, 54, 61-65.

29. Armitage E.L. ; *Stained glass: History, technology and practice* ; Brandford C.T. 1959.

30. Glover, I.C.; Henderson, J. Early glass in South and South-East Asia, China and South-East Asia. *Art Commer. Interact.* 1995, 141-169.

31. Henderson, J.; Chenery, S.; Kröger, J.; Faber, E.W. Glass provenance along the Silk Road: The use of trace element analysis. In *Recent advances in the scientific research on ancient glass and glaze,* Series on Archaeology and History of Science in China*;* Gan, F., Li, Q., Henderson, J., Eds.; World Scientific: Singapore, 2016; Volume 2, pp.17-42.

32. Tamura, T.; Oga, K. Archaeometrical investigation of natron glass excavated in Japan. *Microchem. J.* 2016,126, 7-17.

33. Zhang, Z., Ma, Q. Faience beads of the western Zhou Dynasty excavated in Gansu province, China: A technical study. In *Ancient Glass Research along the Silk Road;* Gan, F.X., Brill, R., Tian, S. Eds.; World Scientific: Singapore, 2009; pp. 275-289.

34. Dussubieux, L.; Kusimba, C.M.; Gogte, V.; Kusimba, S.B.; Gratuze, B.; Oka, R. The trading of ancient glass beads: new analytical data from South Asian and East African soda-alumina glass beads. *Archaeom.* 2008, 50, 797-821.

35. Colomban, Ph.; Khoi, D.N.; Liem, N.Q.; Roche, C.; Sagon, G. Sa Huynh and Cham potteries: microstructure and likely processing. *J. Cult. Herit.*2004, 5, 149-155.

36.Gan, F.; Li, Q.; Henderson, J. eds. *Recent Advances in the Scientific Research on Ancient Glass and Glaze*, Series on Archaeology and History of Science in China, Vol. 2; World Scientific: Singapore, 2016.

37. Saminpanya, S.; Bavornyospiwat, N.; Homklin ,S.;Danyutthapolchai, S.; Bupparenoo, P. () Physical and chemical properties of the ancient glass beads from the highland log-coffin culture and the lowland areas, Thailand: Considerations on their colors and technology. *J. Archaeol. Sci. Rep.* 2016, 8, 366-380.

38. Bouzougar, A.; Barton, N.; Vanhaeren, M.; D'Errico, F. 82,000-year-old shell beads from North Africa and implications for the origins of modern Human behaviour. *Proceedings of the NAS USA* 2007, 104 (24), 9964-9969.

39. Holden, C. Oldest beads suggest early symbolic behaviour. *Sci.* 2004, 304 (5669), 369.

40. Abraham, S.A. Glass beads and glass production in early south India: Contextualizing Indo-Pacific bead manufacture. *Archaeol. Res. Asia* 2016, 6, 4-15.

41. Carter, A.K.; Abraham, S.A.; Kelly, G.O. Updating Asia's Maritime Bead Trade: An Introduction. *Archaeol. Res. Asia* 2016, 6, 1-3.

42. Kelly, G.O. Heterodoxy, orthodoxy and communities of practice: Stone bead and ornament production in Early Historic South India (c. 400 BCE–400 CE). *Archaeol. Res. Asia* 2016, 30-50.

43. Wood, M. Glass beads from pre-European contact sub-Saharan Africa: Peter Francis's work revisited and updated. *Archaeol. Res. Asia* 2016, 6, 65-80.

44. Wood, M.; Panighello, S.; Orsega, E.F.; Robertshaw, P.; van Elteren, J.T.; Crowther, A.; Horton, M.; Boivin, N. Zanzibar and Indian Ocean trade in the first millennium Ce: the glass bead evidence. *Archaeol. Anthropol. Sci.*2016, DOI: 10.1007/s12520-015-0310-z.

45. Van der Sleen, W.G.N. *A Handbook on Beads;* Liberty Cap Books: PA, York, 1973.

46. Freestone, I.C. The provenance of ancient glass through compositional analysis, *Materials Research Society Symposium Proceedings* 2005, 852, 1-14.

47. Colomban, Ph.; Tournié, A. On-site Raman Identification and Dating of Ancient/Modern Stained Glasses at the Sainte-Chapelle, Paris. *J. Cult. Herit.* 2007, 8 (3), 242-256.

48. Degryse, P. *Glass making in the Graeco-Roman world*; Leuven University Press: Leuven, 2014.

49. Foy, D. ; Nenna, M,D. Echanges et commerce du verre dans le monde antique. In *Monographies instrumentum* 24, Actes du Colloque de L'Association Française pour l'Archéologie du Verre (AFAV), Aix-en-Provence-Marseille, 7-9 juin 2001 ; CNRS-mmsh-Université : Aix-Marseille ; ISBN 2-907303-72-4.

50. Picon, M., Vichy, M. D'Orient en Occident: l'origine du verre à l'époque romaine et durant le haut Moyen Age. In *Échanges et commerce du verre dans le monde antique Monographies instrumentum* 24, Actes du Colloque de L'Association Française pour l'Archéologie du Verre (AFAV), Aix-en-Provence-Marseille, 7-9 juin 2001 ; CNRS-mmsh-Université: Aix-Marseille, 2003; ISBN 2-907303-72-4, pp. 17-31.

51. Valooto, M.; Verità, M. Glasses from Pompei, Herculaneum, and the sand of the rivers Belus and Volturno. *Studi della Soprintendenza archeologica di Pompei* 2002, 6, 63-73.

52. Bertran, H. *Nouveau Manuel Complet de la Peinture sur Verre, sur Porcelaine et sur Email* , Encyclopédie-Roret-Ed ; Mulo L : Paris, 1913.

53. Brisac, C. *A thousand years of stained glass;* Book Sales, Macdonald, 1986.

54. Cappa, G, *Le génie verrier de l'Europe. Témoignages de l'Historicisme à la Modernité (1840–1998)*, 2nd ed. ; Mardaga : Liège, 1991.

55. Bontemps, G. *Guide du Verrier – Traité historique et pratique de la fabrication des verres, cristaux, vitraux ;* Librairie du Dictionnaire des Arts Manufacturés : Paris, 1868.

56. Colomban, Ph. The destructive/non-destructive identification of enamels, pottery, glass artifacts and associated pigments – A brief overview. *Arts* 2013, 2, 77-110.

57. Eppler, R.A.; Eppler, D.F. *Glazes and Glass Coatings*. The American Ceramic Society: Westerville, 2000.

58. Nassau, K. *The physics and Chemistry of color,* 2nd ed.; Wiley-VCH: New York, 2001. ibidem *Color for Science, Art and Technology*. Elsevier, 1997.

59. Tilley, R. *Colour and the optical properties of materials;* Wiley and Sons: Chichester, 2000.

60. Colomban, Ph.; Sagon, G.; Faurel, X. Differentiation of antique ceramics from the Raman spectra of their coloured glazes and paintings. *J. Raman. Spectrosc.*2001, 32, 351-360.

61. Colomban, Ph. The use of metal nanoparticles to produce yellow, red and iridescent colour, from Bronze Age to present times in lustre pottery and glass: Solid State Chemistry, Spectroscopy and Nanostructure. *J. Nano Res.* 2009, 8, 109-132.

62. Berke, H.; Wiedemann, H.G. The chemistry and fabrication of anthropogenic pigments Chinese blue and purple in ancient China. *East Asian Sci. Technol. Med.* 2000, 17, 94–120.

63. Colomban, Ph.; Tournié, A.; Ricciardi, P. Raman spectroscopy of copper nanoparticle-containing glass matrices: ancient red stained-glass windows. *J. Raman. Spectrosc.*2009, 40, 1949-1955.

64. Fornacelli, C.; Colomban, Ph.; Turbanti,Memmi I. Toward a Raman/FORS discrimination between Art Nouveau and contemporary stained glasses from CdS_xSe_{1-x} nanoparticles signatures. *J. Raman. Spectrosc.*2015, 46(11), 1129-1139.

65. Bead Researcher Society, (compiled by K. Karklins), https://beadresearch.org/wp-content/uploads/2016/08/Africa.pdf, accessed 7th November 2016)

66. Koleini, F.; Prinsloo, L.C.; Biemond ,W.M.; Colomban, Ph.; Nego, A.; Boeyens, J.; van der Ryst ,M. Towards refining the classification of glass trade beads imported into southern Africa from the 8th to the 16th century AD. *J. Cult. Herit.* 2016, 19, 435-444.

67. Koleini, F.; Prinsloo, L.C.; Biemond, W.; Colomban, Ph.; Ngo, A.T.; Boeyens, J.; Van der Ryst, M.M.; van Brakel, K. Glass trade on Magoro Hill, an archaeological site in southern Africa: glass types and pigments. *Heritage Sci.* 2016, 4:43, 1-20.

68. Koleini, F.; Colomban, Ph.; Antonites, A.; Pikirayi, I; Raman and XRF classification of Asian and European glass beads recovered at Mutamba, a southern African Middle Iron Age site. *J. Archaeol. Sci.: Reports* 2017, 13, 333-340.

69. Koleini, F.; Pikirayi, I.; Colomban, Ph. Revisiting Baranda: a multi-analytical approach in classifying sixteenth/seventeenth-century glass beads from northern Zimbabwe. *Antiquity* 2017, 91 (357), 751–764.

70. Koleini, F.; Machiridza, L.H.; Pikirayi, I.; Colomban, P. The chronology of Insiza cluster Khami-phase sites in south-western Zimbabwe: compositional insights from pXRF and Raman analysis of excavated exotic glass finds. *Archaeom.* 2019, doi: 10.1111/arcm.12463.

71. Beck, H.C. The beads of Mapungubwe District. In *Mapungubwe I;* Fouché, L. Ed.; Cambridge University Press: Cambridge, 1937; pp.104-113.

72. Malleret, L. Classification et nomenclature des « perles » archéologiques en fonction de la symétrie minérale. *Bulletin de l'Ecole française d'Extrême-Orient* 1949, 51(1), 117-124.

73. Van Riet Lowe, C. *The glass beads of Mapungubwe,* Archaeological Series 9; Archaeological Survey: Union of South Africa, 1955.

74. Kidd, K.E.; Kidd, M.A. A classification system for glass beads for the use of field archaeologists. In *Proceedings of the 1982 Glass Trade Bead Conference*, Rochester Research Note 16*;* Hayes, C.F. III Ed.; Rochester Museum and Science Center: New York, NY, 1983; pp. 219-257.

75. Karklins, K. *Glass Beads. Studies in archaeology, architecture and history;* Parks Canada: Ottawa, Ontario, 1985.

76. Davidson, C.C.; Clark, J.D. Trade wind beads: an interim report of chemical studies. *Azania* 1974, 9, 75-86.

77. Buratti, M. Le symbolisme des couleurs dans les productions perlées du Cameroun. In *Les couleurs dans les arts d'Afrique. De la Préhistoire à nos jours ;* Gutierrez, M., Buratti, M., Valentin, M., Ballinger, M., Eds. ; Editions des Archives Contemporaines : Paris, 2016 ; pp. 67-82.

78. *DAACS, Cataloging Manual Beads.* Retrieved from *http://www.daacs.org/wp-content/uploads/2016/10/DAACSBeadManual.pdf*

79. Decorse, C.R. Beads as chronological indicators in West African archaeology: a re-examination. *Beads: J. Soc. Beads Res.* 1989, 1, 41-53.

80. Saitowitz, S.J.; Reid, D.L.; van der Merwe, N.J. Bead trade from Islamic Egypt to South Africa c. AD 900-1250. *S. Afr. J. Sci.* 1996, 92, 101-104.

81. Saitowitz, S.J.; Sampson, C.G. Glass trade beads from rock shelters in the upper Karoo. *S. Afr. Archaeol. Bull.*1992, 47, 94-103.

82. Wood, M. Glass beads and Pre-European trade in the Shashe-Limpopo-region. Master of Arts dissertation, University of the Witwatersrand, Johannesburg, 2005.

83. Wood, M. A glass bead sequence for Southern Africa from the 8th to the 16th century AD. *J. Afr. Archaeol.* 2011, 9, 67-84.

84.Wood, M. Interconnections; Glass beads and trade in southern and eastern Africa and the Indian Ocean – 7th to 16th centuries AD. PhD dissertation, Uppsala University, 2012.

85. Robertshaw, P.; Wood, M.; Melchiorre, E.; Popelka-Filcoff, R.S.; Glascock, M.D. Southern African glass beads: chemistry, glass sources and patterns of trade. *J. Archaeol. Sci.* 2010, 37, 1898-1912.

86. Wood, M.; Dussubieux, L.; Robertshaw, P. Glass finds from Chibuene, a 6th to 17th century AD port in southern Mozambique. *S. Afr. Archaeol. Bull.* 2012, 67, 59–74.

87. Rousaki, A.; Coccato, A.; Verhaeghe, C.; Clist, B.O.; Bostoen, K.; Vandenabeele, P.; Moens, L. Combined spectroscopic analysis of beads from the tombs of Kindoki, Lower Congo Province (Democratic Republic of the Congo). *Appl. Spectrosc.*. 2016, 70(1), 76-93.

88. Coccato, A. ;Costa ,M.; Rousaki, A.; Clist, B.O.; Karklins, K.; Bostoen, K.; Manhita, A.; Cardoso, A.; Dias, C.B.; Candeias, A.; Moens, L.; Mirãob, J.; Vandenabeele, P. Micro-Raman spectroscopy and complementary techniques (hXRF, VP-SEM-EDS, μ-FTIR and Py-GC/MS) applied to the study of beads from the Kongo Kingdom (Democratic Republic of the Congo). *J. Raman. Spectrosc.* 2017, 48, 1468–1478.

89. Babalola, A.B. Ancient history of technology in West Africa: The Indigenous Glass/Glass Bead Industry and the Society in Early Ile-Ife, Southwest Nigeria. *J. Black Stud.* 2017, 48(5), 501-527.

90. Pollard, A.M.; Heron, C. *Archaeological Chemistry*; Royal Society of Chemistry: Cambridge, 1996.

91. Fouché, L. *Mapungubwe: Ancient Bantu Civilization on the Limpopo. Reports on excavations at Mapungubwe* ; Cambridge University Press : Cambridge, 1937.

92. Bonneau, A. ; Moreau, J.F.; Auger, R. ; Hancock, R.G.V. ; Émard, B. Analyses physico-chimiques des perles de traite en verre de facture européenne : quelles instrumentations pour quels résultats ? *Archéologiques* 2014, 26, 109-132.

93. Colomban, Ph. Analyse non destructive des objets d'art par méthodes spectroscopiques portables. *Techniques de l'Ingénieur* 2012, RE 217, 1-12.

94. Colomban, Ph. The on-site/remote Raman analysis with portable instruments - A review of drawbacks and success in Cultural Heritage studies and other associated fields. *J. Raman. Spectrosc.*2012, 43(11), 1529-1535.

95. Bellina, B. Maritime Silk Roads' Ornament Industries: Socio-political Practices and Cultural Transfers in the South China Sea. *Cambridge Archaeol. J.* 2014, 24(3), 345-377.

96. Neri, E.; Morvan, C.; Colomban, Ph.; Guerra, M. F.; Prigent, V. Late Roman and Byzantine Mosaic opaque "Glass-ceramics" *Tesserae* (5^{th}-9^{th} century). *Ceram. Int.* 2016, 42, 18859-18869.

97. Fischbach, N.; Ngo, A.T.; Colomban, Ph.; Pauly, M. Beads excavated from *Antsiraka Boira* necropolis (Mayotte Island, 12^{th}-13^{th} century); Colouring agents and glass matrix composition comparison with contemporary Southern Africa sites. *Revue d'Archéomètrie Archéosciences* 2016, 40, 83-102.

98. Vicenzi, E.P.; Eggins, S.; Logan, A.; Wysoczanski, R. Microbeam characterization of Corning archaeological references glasses. New additions to the Smithsonian microbeam standard collection. *J. Res. Natl. Inst. Stand. Technol.* 2002, 107, 719-727.

99. Simsek, G.; Colomban, Ph.; Casadio, F.; Bellot-Gurlet, L.; Faber, K.; Zelleke, G.; Milande, V.; Tilliard, L. On-site identification of early Böttger red stonewares using portable XRF/Raman instruments: 2 glaze and gilding analysis. *J. American Ceram. Soc.* 2015, 98(10), 3006-3013.

100. Degryse, P.; Henderson, J.; Hodgins, G. *Isotopes in vitreous materials*; Leuven University Press: Leuven, 2009.

101. Dussubieux, L.; Gratuze, B.; Blet-Lemarquand, M. Mineral soda alumina glass: occurrence and meaning. *J. Archaeol. Sci.*2010, 37, 1646-1655.

102. Yuan, H. L.; Gao, S.; Liu, X. M. Accurate U-Pb age and trace element determinations of zircon by laser ablation-inductively coupled plasma- mass spectrometry. *Geostand. Geoanal. Res.* 2004, 28, 353−370.

103. Koch, J.; Günther, D. Review of the State-of-the-Art of Laser Ablation Inductively Coupled Plasmarometry. *Appl. Spectrosc.*2011, 65 (5), 155A-162A.

104. Fotakis, C.; Anglos, D.; Zafiropulos, V.; Georgiou, S.; Tornar, V. *Lasers in the Preservation of Cultural Heritage: Principles and Applications*; CRC Press: Boca Raton, FL, 2006.

105. Miziolek, A.W.; Palleschi, V.; Schechte, I. *Laser Induced Breakdown Spectroscopy*; Cambridge University Press: Cambridge, 2006.

106. Gaudiuso, R.; Dell'Aglio, M.; De Pascale, O.; Senesi G.S.; De Giacomo, A. Laser Induced Breakdown Spectroscopy for elemental analysis in environmental, cultural heritage and space applications: a review of methods and results. *Sens.* 2010, 10(8), 7434-7468.

107. Gouadec, G.; Colomban, Ph. Raman Spectroscopy of nanomaterials: How spectra relate to disorder, particle size and mechanical properties. *Prog. Cryst. Growth and Charact. Mater.* 2007, 53(1), 1–56.

108. Beny, C. ; Prevosteau, J.M. ; Delhaye, M. Applications de la microsonde Raman Mole aux sciences de la Terre. *L'actualité Chimique* 1980, 71, 41-43.

109. Colomban, Ph. Polymerisation degree and Raman identification of ancient glasses used for jewellery, ceramics enamels and mosaics. *J. Non-Cryst. Solids* 2003, 323 (1-3), 180-187.

110. Colomban, Ph. On-site identification and dating of ancient glasses: a review of procedures and tools. *J. Cult. Herit.* 2008, 9 (Suppl.), e55-e60.

111. Colomban, Ph. Non-destructive Raman analysis of ancient glasses and glazes. In *Modern Methods for Analysing Archaeological and Historical Glass*, 1st ed.*;* Janssens, K. Ed.; John Wiley & Sons Ltd, 2013; pp. 275-300.

112. Colomban, Ph., Prinsloo, L.C. Optical spectroscopy of silicates and glasses. In *Spectroscopic properties of inorganic and organometallic compounds: Techniques, Materials and Applications*; Yarwood, J., Douthwaite, R., Duckett, S, Eds.; RSC Publishing: London, 2009; volume 40.

113. Colomban, Ph.; Tournié, A.; Bellot-Gurlet, L. Raman identification of glassy silicates used in ceramics, glass and jewellery: a tentative differentiation guide. *J. Raman. Spectrosc.* 2006,37, 841–852.

114. Prinsloo, L.C.; Colomban, Ph. A Raman spectroscopic study of the Mapungubwe oblates: glass trade beads excavated at an Iron Age archaeological site in South Africa. *J. Raman. Spectrosc.* 2008, 39, 79-90.

115. Prinsloo, L.C.; Boeyens, J.C.A.; Van der Ryst, M.M.; Webb, G. Raman signatures of the modern pigment (Zn,Cd)$S_{1-\chi}Se_{\chi}$ and glass matrix of a red bead from Magoro Hill, an archaeological site in Limpopo Province, South Africa, recalibrate the settlement chronology. *J. Mol. Struct.* 2012, 1023, 123-127.

116. Prinsloo, L.C.; Tournié, A.; Colomban, Ph. A Raman spectroscopic study of glass trade beads excavated at Mapungubwe hill and K2, two archaeological sites in southern Africa, raises questions about the last occupation date of the hill. *J. Archaeol. Sci.*2011, 38, 3264-3277.
Title of Site. Available online: URL (accessed on Day Month Year).

117. Tournié, A.; Prinsloo, L.C.; Colomban, Ph. Raman spectra database of the glass beads excavated on Mapungubwe Hill and K2, two archaeological sites in South Africa. University of Petroria, 2010; Retrieved from https://hal.archives-ouvertes.fr/hal-00543867/document, https://arxiv.org/ftp/arxiv/papers/1012/1012.1465.pdf (access 03/06/2015)

118. Tournié, A.; Prinsloo, L.C.; Colomban, Ph. Raman classification of glass beads excavated on Mapungubwe hill and K2, two archaeological sites in South Africa. *J. Raman. Spectrosc.* 2011, 43, 532-542.

119. Caggiani, M.C.; Colomban, Ph. Raman identification of strongly absorbing phases: the ceramic black pigments. *J. Raman. Spectrosc.* 2011, 42 (4), 839-843.

120. Huffman, T. *Handbook to the Iron Age*; University of KwaZulu-Natal Press: Scotville, 2007.

121. Robertshaw, P.; Rasoarifetra, B.; Wood, M.; Melchiorre, E.; Popelka-Filcoff, R.S.; Glascock, M.D. Chemical analysis of glass beads from Madagascar. *J. Afr. Archaeol.* 2006, 4, 91-109.

122. Simsek, G.; Colomban, Ph. New investigation on glass beads from the necropolis of Vohemar, Northern Madagascar. (unpublished).

123. Robertshaw, P.; Wood, M.; Haour, A. Chemical analysis, chronology, and context of a European glass bead assemblage from Garumele, Niger. *J. Archaeol. Sci.* 2014, 41. 591-604.

124. Cagno, S.; Brondi Badano, M.; Mathis, F.; Strivay, D.; Janssen, K. Study of medieval glass from Savona (Italy) and their relation with the glass produced in Altare. *J. Archaeol. Sci.*2012, 39 (7), 2191-2197.

125. Dussubieux, L.; Karklins, K. Glass bead production in Europe during the 17th century/ Elemental analysis of glass materials found in London and Amsterdam. *J. Archaeol. Sci. Reports* 2016, 5; 574-579,

126. Robertshaw, P.; Magnavita, S.; Wood, M.; Melchiorre, E.; Popelka-Filcoff, R.; Glascock, M.D. Glass beads from Kissi (Burkina Faso): chemical analysis and archaeological interpretation. In *Crossroads: Cultural and technological developments in first millennium BC / AD West Afric*a; Magnavita, S., Koté, L., Breunig, P., Idé, O.A. Eds.; *J. African Archaeology*, Monograph Series 2; Africa Magna Verlag: Frankfurt am Main, 2009; pp. 105–118.

127. Colomban, Ph.; Truong, C. Non-destructive Raman study of the glazing technique in lustre potteries and faience (9–14th centuries): silver ions, nanoclusters, microstructure and processing. *J. Raman. Spectrosc.*2004, 35, 195–207.

128. Tite, M.; Pradell, T.; Shortland, A. () Discovery, production and use of tin-based opacifiers in glasses, enamels and glazes from the late iron age onwards: a reassessment. *Archaeom.* 2008, 50, 67-84.

129. Pages-Camagna, S.; Colinart, S.; Coupry, C. Fabrication process of archaeological Egyptian blue and green pigments enlightened by Raman microscopy and scanning electron microscopy. *J. Raman. Spectrosc.* 1999, 30 (4), 313-317.

130. Cheng, X.; Yin, X.; Ma, Y.; Lei, Y. Three fabricated pigments (Han purple, indigo and emerald green) in ancient Chinese artifacts studied by Raman microscopy, energy-dispersive X-ray spectrometry and polarized light microscopy. *J. Raman. Spectrosc.* 2007, 38. 1274–1280.

131. Lei, Y.; Xia, Y. Study on production techniques and provenance of faience beads excavated in China. *J. Archaeol. Sci.* 2015, 53, 32-42.

132. Kirmizi, B.; Gokturk, H.; Colomban, Ph. Colouring Agents in the Pottery Glazes of Western Anatolia: A New Evidence for the Use of Naples Yellow Pigment Variations during the Late Byzantine Period. *Archaeom.*2015, 57 (3), 476-496.

133. Rosi, F.; Miliani, C.; Brunetti, B.G.; Sgamellotti, A.; Grygar, T.; Hradil, D. Raman scattering features of lead pyroantimonate compounds. Part I: XRD and Raman characterization of $Pb_2Sb_2O_7$ doped with tin and zinc. *J. Raman. Spectrosc.* 2009, 40 (1), 107-11.

134. Rosi, F.; Manuali, V.; Grygar, T.; Bezdicka, P.; Brunetti, B.G.; Sgamellotti, A., Burgio, L.; Seccaronif, C.; Miliani, C. Raman scattering features of lead pyroantimonate compounds: implication for the non-invasive identification of yellow pigments on ancient ceramics. Part II. In situ characterisation of Renaissance plates by portable micro-Raman and XRF studies. *J. Raman. Spectrosc.*2011, 42 (3), 407-414.

135. Faurel, X.; Vanderperre, A.; Colomban, Ph. Pink Pigment optimisation by resonance Raman Spectroscopy. *J. Raman. Spectrosc.* 2003, 34(4), 290-294.

136. Davison, C.C. Chemical resemblance of garden roller and M1 glass beads. *Afr. Stud.* 1973, 32(4), 247-257.

137. Gardner, G.A. *Mapungubwe II*; J.L. van Schaik: Pretoria, 1963.

138. Carey, M. Powder-glass beads in Africa. In *Ornaments from the Past: beads studies after Beck;* Glover, I., Hughes-Brock, H., Henderson, J. Eds.; The Bead Study Trust: London, 2003; pp. 108-114.

139. Opper, M.J.; Opper, H. Powdered-glass beads and beads trade in Mauritania. Beads: *J. Soc. Bead Res.* 1993, 5, 37-54.

140. Simak, E. Traditional Mauritanian Powder-glass Kiffa beads. *Ornam.* 2006, 29 (5), 50-54.

141. Haigh, J. Present-day bead-making in Ghana. In *Ornaments from the Past: Bead studies after Beck;* Glover, I., Hughes-Brock, H., Henderson, J., Eds.; The bead Study Trust, 2003; pp. 115-117.

142. Lankton, J.W.; Ige, O.A.; Rehren, Th. Early primary glass production in Southern Nigeria. *J. Afr. Archaeol.* 2006, 4, 111-138.

143. Brill, R.H.; Stapleton, C.P. *Chemical Analyses of Early Glasses*, Volume 3; Corning Museum: New York, 2012.

144. Wedepohl, K.H.; Simon, K.; Kronz, A. Data on 61 chemical elements for the characterization of three major glass compositions in late antiquity and the middle ages. *Archaeom.* 2011, *53*, 81-102.

145. Koleini, F., Colomban, P., Pikirayi, I. Post-15th century European glass beads in southern Africa: Identification, composition and classification using pXRF and Raman spectroscopy. (under review).

146. Colomban, Ph. Rocks as blue, green and black pigments/dyes of glazed pottery and enamelled glass artefacts – A review. *Eur. J. Mineral.* 2013, 25, 863-879.

147. Gratuze, B.; Soulier, I.; Barrandon, J.N.; Foy, D. De l'origine du cobalt dans les verres". *Revue d'archéométrie* 1992, 16, 97-108.

148. Gratuze, B. ; Soulier, I. ; Blet, M. ; Vallauri, L. De l'origine du cobalt: du verre a` la céramique. *Revue d'archéométrie* 1996, 20, 77-104.

149. Gronenborn, D. Beads and the emergence of the Islamic slave trade in the southern Chad basin (Nigeria). Beads: *J. Soc. Beads Res.* 2009, 21, 47-51.

150. Guerrero, S. Venetian glass beads and the slave trade from Liverpool, 1750-1800, *Beads: J. Soc. Beads Res.* 2010, 22, 52-70.

151. Pallaver, K. A recognized currency in beads: glass beads as money in 19th century East Africa: the Central Caravan road. In *Money in Africa;* Catherine, E., Fuller, H., Perkins, J. Eds.; The British Museum: London, 2009; pp. 20-29.

152. Euba, O. Of blue beads and red; the role of Ife in the West African trade in Kori beads. *J. Historical Soc. Niger.* 1982, 11 (1/2), 109-127.

FIGURE CAPTIONS

Fig. 1 Variety of the glass flux compositions expressed in the Na_2O-K_2O-CaO relative ratio.

Fig. 2 Bead selection illustrating the variety of shape (tube, cylinder, oblate, minute, mold (e10), etc.) and colour. a) K2-IP series (1-3). (1) turquoise blue, tube (Mutamba), (2-3) blue-green, tube (Basinghall). EC-IP series (4-7). (4) brownish red, tube (5) black, cylinder (Mutamba), (6) black, tube (Basinghall), (7) cobalt blue with Malayite, oblate, wound (Magoro Hill); b) Mapungubwe Oblate (1-6) (Mutamba); c) Khami-IP series (1-7). (1) light green, cylinder (Basinghall), (2-3) yellow, cylinder, oblate (Baranda), (4) green (Basinghall), (5-6) green, oblate (Baranda), (7) white, tube (Baranda), (8) green recycled glass bead, tube (Basinghall); d) Khami-IP series (1-8). (1-2) brownish red, oblate, tube (Baranda), (3) light blue, cylinder (Basinghall), (4-6) cobalt blue, oblate (Baranda), (7-8) white, oblate, cylinder (Baranda); e) European beads with lead arsenate in composition (1-9). (1-2) white, oblate (Baranda). (3-9) found at Magoro Hill. (3) coblat blue, tube (4) light blue, oblate (5-6) green, tube, cylinder (7) white heart, oblate (8) compound bead, sphere, (9) brick red, cylinder. European Soda-rich plant ash (10-11), (10) brownish red on gray (Parma), (11) green heart (Mapungubwe).; f) European beads (1-9). 1) high potash and low phosphate glass, simple-small hexagonal (K2), 2) synthetic soda glass, annular (K2) (3) high potash and phosphate glass, compound-large hexagonal (K2) (4) high alumina soda glass with Levantine ash, un-coloured, sphere (Magoro Hill), (5) coblat blue with calcium antimoniate as opacifier, cylinder (Mutamba), (6) light blue, oblate (Magoro Hill), (7) white, cylinder (Magoro Hill), (8) white. cylinder, (Magoro Hill), (9-10) lead arsenate glass, striped (Mapungubwe), 10) pink, oblate, 11) Red $(Zn,Cd)S_xSe_{x-1}$, sphere, moulded.

Fig. 3 Schematic of the bead series according Wood' morphological classification [67,82,84]. Corresponding composition type and colour palette are given (see text).

Fig. 4 Map shows the sites referred to in the paper

Fig. 5 Al-Ca-Mg+K oxides ratio diagram highlighting the different types of glass (h: high; l: low). The symbols used for each series are given. Dashed lines and solid delimit main soda-lime plant ash glass and soda compositions.

Fig. 6 Representative Raman signatures of: 1) soda glass of IP series; 2) soda glass with high iron content uses as colorant; 3) soda/lime glass of Mapungubwe oblate, some of Khami-IP series and European beads; 4) soda/lime glass with high iron content (mostly recorded for green and yellow Khami-IP series); 5) soda/lime glass, recorded on European beads with high potassium; 6) lead arsenate glass, European beads. A baseline has been subtracted according to the procedure described in Colomban [110].

Fig. 7 The plot of Si-O bending vs stretching vibration of glass beads found at southern Africa, classifying the different glass series. Basinghall Farm (light blue), Baranda Farm (dark blue), Magoro Hill (brownish-red) and Mutamba (yellow).

Fig. 8 Representative Raman signatures of pigments, opacifiers and secondary phases: 1) Fe-S chromophore in black IP series; 2) Fe-S chromophore with an extra peak at 355 cm^{-1} that shows a high concentration of the chromophore (IP series); 3) Fe-S chromophore in black Mapungubwe Oblate. (Mutamba); 4) Manganese oxide (Jacobsite) in black European bead (Magoro Hill); 5) calcium antimonitae ($CaSb_2O_6$) used as white pigment in a white European beads (Baranda); 6) calcium antimonitae ($CaSb_2O_7$ and $CaSb_2O_6$) in one European beads (Magoro Hill); 7) Malayite in one cobalt blue bead (Magoro Hill); 8) Tin oxide used as opacfier in Mapungubwe Oblate (Mutamba); 10) calcium carbonate impurity in a recycled glass bead (Basinghall); 11) Pb-Sn-Sb triple oxide in European beads (Magoro Hill); 12) Lead tin yellow (II) detected in Khami-IP and Mapungubwe series; 13) a mix of lead tin yellow (II) and lead oxide in orange Mapungubwe oblate and Khami-IP; 14) Lazurite in blue European beads (Magoro Hill).

Fig. 9 Example of recycled bead (local production): SEM-EDX element mapping highlights the mixture of soda- and potash-glass grains.

Table 1 Glass types, main characteristics and origin/period

Flux	Glass type	Sub-groups	Average oxide content wt%					Expected Alkali source	Period	Expected Origin
			Na_2O	K_2O	CaO	MgO	PbO			
Na	Soda	low Al							>2AD	South Asia, South-East Asia
		high Al (Al_2O_3:4-10)	15-20	1.5-2.5	2-4	0.2-1		?	> 1BC~-6AD	
									9-19AD	South Asia
		Venetian cristallo Façon de Venise	12-15	2-4	4-10	1-3		ashes	16AD-18AD	Europe
	Soda Lime	low Al, high Mg	8-20	0-3	3-10	2-10		Plant ashes	>15BC-8BC	Near East
		low Al, low Mg	13-20	0-1	5-10	0-1		Natron	>8BC-3AD	Roman Levant (no Sb_2O_3)
		Low Al,low Mg, High Sb	15-20	0-1	4-6	0-1		Natron	1AD-3AD	Mediterranean area
		High Fe-Mg	16-20	0-1	5-10	1-2		Natron	3AD-5AD	Mediterranean area, Europe
		Levantine glass	10-15	0-1	8-12	0-1		Natron	5AD-8AD	
		High Mg early Islamic glass	10-18	1-3	6-12	3-7		Natron & Plant ashes	9AD-10AD	Islamic world
		Modern	10-20	0-1	10-20	0-1		Synthetic soda	19AD ->	Worldwide

K	potash	Low Mg High K	0-8	8-18	0-4	0-1		Plant ashes	Bronze Age	Europe
		high Al							>1BC	Vietnam, South China
		medium Al								South Asia
		High K European Glass	0-8	8-18	6-20	0-5		Plant ashes	>8 AD	West Europe
		High Lime low Alkali	<10	<12	15-20	0-1		Plant ashes (oak)	15AD-17AD	Northern Europe
Na-K	Mixed	Mixed Alkali Glass	5-10	5-10	10	2-6		Plant ashes (seaweed)	16-17	Northern Europe
Pb	Lead	high Ba							>3BC	China
		high Na							>1AD	China
		High Na							>2BC	Roman
		High-Lead Islamic Glass	8-10	0-2	4-5	0-1	30-40	Natron & Plant ashes	10-14AD	Islamic world
		High-Lead Medieval Glass	0-1	3-10	4-16	1-3	20-65	Plant ashes	8-14AD	Europe

Table 2 Main opacifying and colouring agents

Colour	Elements	Phase	Raman detected	Period	Remarks
White		bubbles	yes		
	Si	quartz (SiO_2)	yes		
	Ti	rutile,anatase (TiO_2)	yes		
	Zr	zircon ($ZrSiO_4$),zirconia (ZrO_2)	yes	>20th	
	P	apatite ($Ca_3(PO_4)_2$)	yes	Antiquity	bones
	Ca	calcite ($CaCO_3$)	yes	Antiquity	
	Sb	antimonate ($CaSb_2O_7$)	yes		
	Sb	antimonate ($CaSb_2O_6$)	yes		
	Sn	cassiterite (SnO_2)	yes	>5AD	
	As	Arsenate $(Ca,Pb)_{1.5}AsO_4$	yes	>17th, >18th	
Blue	Cu	Egyptian blue ($CaCuSi_4O_{10}$)	yes	>3000BC	
	Ba,Cu	Han blue ($BaCuSi_4O_{10}$)	yes	>500BC	
	Ba,Cu	Han violet ($BaCuSi_2O_6$)	yes	>200BC	
	Cu	dissolved Cu^{2+}	no		turquoise in alkali glass matrix
	S	Lazurite ($Na_8[Al_6Si_6O_{24}]S_n$)	yes	>1BC	
		ultramarine	yes	>19th	
	Co	dissolved Co^{2+}	Indirectly		
		spinels $(Co,Cr,X)AlO_4$	yes		
		olivine ($CoSiO_2$)	yes	>17th	
		Co oxide (Co_3O_4)			
	V	zircon ($V:ZrSiO_4$)	yes		
Yellow	Fe	Dissolved Fe^{3+}	no		
	Sb	Pyrochlore ($PbSb_{2-x}M_xO_{7-d}$)	yes	>1000BC	Naples yellow
	Sn	$Pb_2Sn_{1-y}M_yO_4$	yes	Antiquity	
	U	Dissolved UO^{2+}			
	Pb	PbO		Antiquity	
	Sn	Sphene ($CaSnSiO_5$)			Malayite

	Zn,Cr	$ZnCrO_4$		>1800	
Green	Cu	Cu^{2+} dissolved	no	Neolithic	
	Cr	Cr^{3+} dissolved	no		
	Cr	Cr_2O_3	yes	1800s	
		$3CaO\ Cr_2O_3\ 3SiO_2$	yes		Victoria green, Malawyte
	Cr,Co	Spinels:$CoCr_2O_4$,$CoTiO_4$	yes		
		Olivine $NiSiO_4$			
Red	Cu	Cu°	indirect	>Neolithic	
	Fe	Haematite	Yes	15AD	
	Au	Au°	indirect	>16AD	

Table 3 A summary on number of published articles about glass beads found in Africa except Egypt and the east and west coast islands of Africa. Compiled by the Society of Bead Researchers [65]

Location	Country (No. of sites)	Percentage
West Africa	Ghana (13), Mauritania (9), Mali (7), Senegal (3), Burkina Fasso, 2, Niger, Sierra Leone; Benin, 2; Nigeria, 12; Guinea, 1	46%
North central Africa	Congo, 3; Cameroon, 1; Angola, 4	7%
Southern Africa	South Africa, Botswana & Namibia, 17; Zimbabwe, 6	21%
East Africa	Kenya, Uganda and Zanzibar, 12; Ethiopia, 7; Madagascar, 3; Sudan, 5; Tanzania, 2	26%

Table 4 Identified/expected local production of glass beads

Type	Place	Date	Remarks	References
Garden Roller	K2 Limpopo Valley, SA	K2 (1100-1220)	Molds found with beads. Big beads are made by sintering/melting smaller ones	[85,114,136,137]
Kiffa beads	Kiffa, Mauritania	19th c.	Made from glass powder	[138-140]
Bodom	Ghana Western Africa	19th c.	Powder-glass	[5,141]
Iyun, Segi	Ife, Nigeria	12th-14th c. 18th c.	Grinding, Powder-glass beads	[152]
	Ile-Ife, Nigeria	11th-15th c.	Glass cake, melting beads, high lime-high alumina, high lime-low alumina, soda-lime.	[142]
	Igbo Olokun, Nigeria	11th-15th c.	Crucible production of High lime-high alumina & low lime-high alumina glass from raw local materials.	[89]
Light green drawn bead	Basinghall (Botswana)	1592-1648	Inhomogeneous glass made by sintering soda, mixed alkali and potash glass.	[66]
Blue beads	Carthage/Utica	1st	Grains + glassy cement	[109]